hep-ph/0310123 IFUP–TH/2003–37 CERN-TH/2003-240

Towards a complete theory of thermal leptogenesis in the SM and MSSM

G.F. Giudice[1], **A. Notari**[2], **M. Raidal**[3], **A. Riotto**[4], **A. Strumia**[5]

[1] *Theoretical Physics Division, CERN, CH-1211 Geneva 23, Switzerland*

[2] *Scuola Normale Superiore, Piazza dei Cavalieri 7, Pisa, I-56126, Italy*

[3] *National Institute of Chemical Physics and Biophysics, Tallinn 10143, Estonia*

[4] *INFN, Sezione di Padova, via Marzolo 8, Padova I-35131, Italy*

[5] *Dipartimento di Fisica dell'Università di Pisa and INFN, Italia*

Abstract

We perform a thorough study of thermal leptogenesis adding finite temperature effects, RGE corrections, scatterings involving gauge bosons and by properly avoiding overcounting on-shell processes. Assuming hierarchical right-handed neutrinos with arbitrary abundancy, successful leptogenesis can be achieved if left-handed neutrinos are lighter than 0.13 eV and right-handed neutrinos heavier than 2×10^7 GeV (SM case, 3σ C.L.). MSSM results are similar. Furthermore, we study how reheating after inflation affects thermal leptogenesis. Assuming that the inflaton reheats SM particles but not directly right-handed neutrinos, we derive the lower bound on the reheating temperature to be $T_{\rm RH} \gtrsim 2 \times 10^9$ GeV. This bound conflicts with the cosmological gravitino bound present in supersymmetric theories. We study some scenarios that avoid this conflict: 'soft leptogenesis', leptogenesis in presence of a large right-handed (s)neutrino abundancy or of a sneutrino condensate.

1 Introduction

If some new physics violates lepton number $\mathcal{L}$ at an energy scale $\Lambda_{\mathcal{L}}$, neutrinos get small Majorana masses via the dimension-5 effective operator $(LH)^2/\Lambda_{\mathcal{L}}$. Experiments suggest $\Lambda_{\mathcal{L}} \sim 10^{14}\,\mathrm{GeV}$. Indeed the solar and atmospheric data can be explained by neutrino oscillations induced by the following neutrino masses and mixings [1]

$$\begin{aligned} |\Delta m^2_{\mathrm{atm}}| &= (2.0^{+0.4}_{-0.3}) \times 10^{-3}\,\mathrm{eV}^2, \quad \sin^2 2\theta_{\mathrm{atm}} = 1.00 \pm 0.04, \\ \Delta m^2_{\mathrm{sun}} &= (7.2 \pm 0.7) \times 10^{-5}\,\mathrm{eV}^2, \quad \tan^2 \theta_{\mathrm{sun}} = 0.44 \pm 0.05. \end{aligned} \tag{1}$$

Experiments will make further progress towards measuring effects accessible at low energy, completely described by 9 Majorana parameters: 3 neutrino masses, 3 mixing angles, 3 CP-violating phases.

One possible mechanism to generate the dimension-5 operator $(LH)^2/\Lambda_{\mathcal{L}}$ is known as 'see-saw' mechanism [2]. Adding three right-handed neutrinos $N_{1,2,3}$ with heavy Majorana masses $m_{N_3} > m_{N_3} > m_{N_1} \gg M_Z$ and Yukawa couplings Y^ν_{ij}

$$\mathscr{L} = \mathscr{L}_{\mathrm{SM}} + \left(\frac{m_{N_i}}{2} N_i^2 + Y^\nu_{ij} L_i N_j H + \mathrm{h.c.} \right), \tag{2}$$

one obtains light neutrino states with Majorana masses $m_\nu = -(vY^\nu)^T\ m_N^{-1}\ (vY^\nu)$. The see-saw is a simple and elegant mechanism, but hard to test experimentally. It predicts no relation between the 9 low-energy parameters, just reproducing them in terms of 18 high-energy ones. The right-handed neutrinos which constitute the essence of the see-saw are too heavy or too weakly coupled to be experimentally observed. There are few possible indirect probes. For instance, in some supersymmetric models the Yukawa couplings Y^ν_{ij} might induce sizable rates for lepton flavour violating processes such as $\mu \to e\gamma$ []. On the cosmological side, *thermal leptogenesis* [3] provides an attractive scenario for the generation of the baryon asymmetry of the universe [4]. The three necessary conditions for the generation of the baryon asymmetry [5] are satisfied in the Standard Model (SM) with additional, heavy singlet right-handed neutrinos: the baryon number is violated by sphaleron processes which convert the lepton asymmetry induced by the Majorana nature of the right-handed neutrino masses into baryon asymmetry; CP-violation is due to the Yukawa interactions of the right-handed neutrinos with the SM lepton doublets and out-of-equilibrium is induced by the right-handed neutrino decays. For some recent analyses see [6, 7, 8, 9].

The goal of this paper is to perform a thorough analysis of thermal leptogenesis within the SM and the Minimal Supersymmetric Standard Model (MSSM). We improve the computation of baryon asymmetry generated through the mechanism of thermal leptogenesis by

i) including finite temperature corrections to propagators, masses, decay and scattering processes, and to the CP-asymmetry;

ii) renormalizing couplings at the relevant scale ($\sim 2\pi T$, where T is the relevant temperature, rather than $\sim M_Z$);

iii) adding $\Delta L = 1$ scatterings involving gauge bosons which turn out to be comparable or larger than the ones involving the top quark included in previous computations;

iv) performing a proper subtraction of washout scatterings mediated by intermediate on-shell particles (once this is correctly done, they are no longer resonantly enhanced);

v) extending the analysis to situations where right-handed (s)neutrinos give a sizable contribution to the total energy density;

vi) discussing how the predictions of thermal leptogenesis depend upon the cosmological assumptions. In particular, we study the effects of reheating after inflation and compute the lowest value of the reheating temperature $T_{\rm RH}$ for successful leptogenesis.

The paper is organized as follows. In section 2 we briefly summarize some general results of field theory at finite temperature. In section 3 we discuss how we include thermal corrections and how they affect the different ingredients of leptogenesis. Details can be found in a series of appendices: Boltzmann equations in appendix A, scattering rates in appendix B, CP-asymmetries in appendices C (SM) and D (MSSM). In section 4 we combine all ingredients to get the final baryon asymmetry predicted within SM leptogenesis, and study which thermal corrections turn out to be numerically important. On the basis of the lesson learned for the SM, in section 5 we address the more involved case of supersymmetric leptogenesis. We apply our improved computation also to the 'soft leptogenesis' scenario [10, 11]. In section 6 we discuss how the baryon asymmetry changes when the maximal temperature reached by the universe after inflation is not much higher than m_{N_1}. The variation depends on one extra parameter, the reheating temperature $T_{\rm RH}$. Finally our results are summarized in section 7.

2 Finite-temperature propagators

In order to consider finite temperature effects in the plasma, we work in the so-called real time formalism (RTF) [12] of thermal field theory. The Green's functions computed in this formalism are directly time-ordered ones. The RTF requires the introduction of a ghost field dual to each physical field leading to the doubling of degrees of freedom. The thermal propagator has therefore a 2×2 structure: the (11) component refers to the physical field, the (22) component to the corresponding ghost field, with the off-diagonal components (12) and (21) mixing them.

Scalars

The complete propagator of a scalar particle (*e.g.* the Higgs) in momentum space is

$$G(K) = \begin{pmatrix} G^{11}(K) & G^{12}(K) \\ G^{21}(K) & G^{22}(K) \end{pmatrix} = U\left(T,K\right) \begin{pmatrix} \Delta_B(K) & 0 \\ 0 & \Delta_B^*(K) \end{pmatrix} U\left(T,K\right) \,, \qquad (3)$$

$$U\left(T,K\right) = \begin{pmatrix} \cosh\theta_K & \sinh\theta_K \\ \sinh\theta_K & \cosh\theta_K \end{pmatrix}, \qquad (4)$$

$$\cosh\theta_K = \sqrt{1+f_B(\omega)}\,, \quad \sinh\theta_K = \sqrt{f_B(\omega)}, \qquad f_B \equiv \frac{1}{e^{|\omega|/T}-1}, \tag{5}$$

where K is the particle four-momentum. In a general frame where the thermal bath has four-velocity U^μ ($U^\mu U_\mu = 1$), we define the Lorentz-invariant quantities

$$\omega \equiv K^\mu U_\mu, \quad k \equiv \sqrt{(K^\mu U_\mu)^2 - K^\mu K_\mu}. \tag{6}$$

These coincide with the particle energy and momentum in the rest frame of the thermal bath, $U^\mu = (1,0,0,0)$.

In Eq. (3), $\Delta_B(K)$ is the resummed propagator

$$\Delta_B(K) = \frac{i}{K^2 - m_B^2 - \Sigma_B(K) + i\epsilon}\,, \tag{7}$$

where m_B is the bare mass and $\Sigma_B(K)$ is the finite-temperature self-energy of the scalar boson field. $\Sigma_B(K)$ describes the continuous interactions with the heat bath altering the propagation of the boson, and it modifies the dispersion relation, substituting particles with quasiparticles. At one-loop the self-energy takes the form $\Sigma_B(K) = \mathrm{Re}\,\Sigma_B(K) + i\,\mathrm{Im}\,\Sigma_B(K)$, where $\mathrm{Re}\,\Sigma_B(K) = m_B^2(T)$ is the effective plasma mass squared and $\mathrm{Im}\,\Sigma_B(K) = -2\,\omega\,\Gamma_B$ is proportional to the damping rate Γ_B of the boson in the plasma. Since $|\mathrm{Im}\,\Sigma_B(K)|$ is suppressed compared to $|\mathrm{Re}\,\Sigma_B(K)|$ [13], in the following we will work with resummed propagators for scalar bosons neglecting the absorptive part. Notice also that since we are considering one-loop thermal corrections to processes where all external fields are physical, we only need the (11) component of the bosonic propagator

$$G^{11}(K) = \cosh^2\theta_K \left(\frac{i}{K^2 - m_B(T)^2 + i\epsilon}\right) + \sinh^2\theta_K \left(\frac{-i}{K^2 - m_B(T)^2 - i\epsilon}\right)\,, \tag{8}$$

where we have included the bare mass in $m_B(T)$. Using the property

$$\frac{1}{x+i\epsilon} = P\left(\frac{1}{x}\right) - i\pi\delta(x)\,, \tag{9}$$

where P denotes the principal value, the propagator can be rewritten as:

$$G^{11}(K) = \frac{i}{K^2 - m_B(T)^2 + i\epsilon} + 2\pi f_B(\omega)\delta\left[K^2 - m_B(T)^2\right]\,. \tag{10}$$

Fermions

The (one-loop) resummed propagators for fermion fields can be written in RTF as

$$S(K) = \begin{pmatrix} S^{11}(K) & S^{12}(K) \\ S^{21}(K) & S^{22}(K) \end{pmatrix} = M\,(T,K) \begin{pmatrix} \Delta_F(K) & 0 \\ 0 & \Delta_F^*(K) \end{pmatrix} M\,(T,K)\,, \tag{11}$$

where

$$M\left(T,K\right)=\left(\begin{array}{cc}\cos\phi_K & -\sin\phi_K\\ \sin\phi_K & \cos\phi_K\end{array}\right) \tag{12}$$

and

$$\cos\phi_K=\left[\theta(\omega)-\theta(-\omega)\right]\sqrt{1-f_F(\omega)}\,,\quad \sin\phi_K=\sqrt{f_F(\omega)},\qquad f_F(\omega)\equiv\frac{1}{e^{|\omega|/T}+1}. \tag{13}$$

In Eq. (11) $\Delta_F(K)$ is the resummed propagator

$$\Delta_F(K)=\frac{i}{\gamma^\mu K_\mu-m_0-\Sigma_F(K)+i\epsilon}\,, \tag{14}$$

where m_0 is the fermion bare mass and $\Sigma_F(K)$ is the self-energy of the boson field at finite temperature. At one-loop the fermionic self-energy is given by [14]

$$\Sigma_F(K)=-a(K)\,\gamma^\mu K_\mu-b(K)\,\gamma^\mu U_\mu\,, \tag{15}$$

where U^μ is the four-velocity of the thermal bath as seen from a general frame. Neglecting the zero-temperature mass m_0, the coefficients $a(K)$ and $b(K)$ are given by

$$a(K) = \frac{m_F^2(T)}{k^2}\left[1+\frac{\omega}{2k}\ln\frac{\omega-k}{\omega+k}+\frac{\omega k}{T^2}I+\frac{k^2}{T^2}J\right], \tag{16}$$

$$b(K) = -\frac{m_F^2(T)}{k}\left[\frac{\omega}{k}+\frac{1}{2}\left(\frac{\omega^2}{k^2}-1\right)\ln\frac{\omega-k}{\omega+k}+\frac{(\omega^2-k^2)}{T^2}I\right], \tag{17}$$

$$I = \int_0^\infty\frac{dp}{\pi^2k^2}\left[f_B(p)+f_F(p)\right]\left[\frac{\omega}{2}\ln\frac{4p(p+k)+k^2-\omega^2}{4p(p-k)+k^2-\omega^2}+p\ln\frac{4p^2-(k+\omega)^2}{4p^2-(k-\omega)^2}\right] \tag{18}$$

$$J = \int_0^\infty\frac{dp}{2\pi^2k}\left[f_B(p)-f_F(p)\right]\ln\frac{4p(p+k)+k^2-\omega^2}{4p(p-k)+k^2-\omega^2}. \tag{19}$$

Here $f_{B,F}$ are the Bose-Einstein and Fermi-Dirac distributions, respectively, and $m_F(T)$ is the effective mass of the fermion in the plasma. Notice that this mass is not a "true" fermionic mass since it does not affect the chiral symmetry. The thermal mass is generated radiatively and comes from terms which are chiral-symmetric in the Lagrangian. The integrals I and J are gauge-dependent and have been computed here in the Feynman gauge. In the high-temperature limit ($T\gg k$), the terms in eqs. (16) and (17) proportional to the integrals I and J can be neglected, as they only give subleading contributions, leaving a result for the coefficients a and b which is gauge independent[1].

For a fermion charged under an SU(N) gauge group with coupling g and having Yukawa coupling Y, the thermal fermionic mass squared is $m_F^2(T)=g^2T^2C(R)/8+N_f\left|Y\right|^2T^2/16$,

[1]Our subsequent computations involve weakly coupled particles, so that m_F^2/T^2 turns out to be small and neglecting I and J is an excellent approximation.

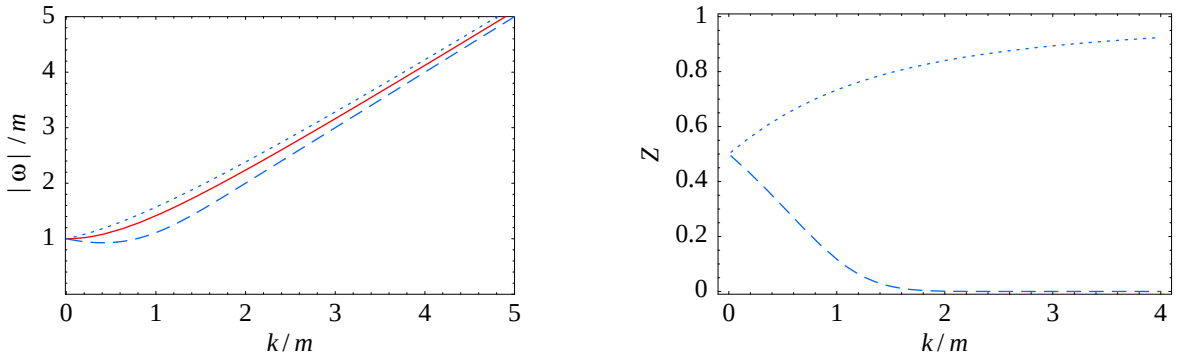

Figure 1: *The dispersion relation $|\omega(k)|$ (fig. 1a) and the residue (fig. 1b) of particle (dotted line) and 'hole' (dashed line) excitations of a fermion with thermal mass m at temperature T for $m \ll T$. The solid line shows the approximation $\omega^2 = m^2 + k^2$.*

where $C(R)$ is the quadratic Casimir of the fermionic representation (*e.g.* $C(R) = (N^2 - 1)/(2N)$, when R is a fundamental of $SU(N)$) and N_f is the particle multiplicity flowing in the loop.

Interactions of the fermions with the thermal bath modify the fermionic dispersion relation [14] leading to two different types of excitations with positive energy: 'particles' and 'holes' with the wrong correlation between chirality and helicity in the bare massless limit. The names 'particles' and 'holes' are suggested by an analogy with superconductors [14]. This is because the propagator in eq. (14) has poles at $\omega = \pm k - b/(1+a)$, an equation with two different positive-energy solutions E_p and E_h ($E = |\omega|$, see fig. 1a). At low-momentum, $k \ll m_F$,

$$E_p = m_F + \frac{k}{3} + \frac{k^2}{3m_F} + \cdots , \qquad E_h = m_F - \frac{k}{3} + \frac{k^2}{3m_F} + \cdots , \tag{20}$$

while at larger momenta $T \gg k \gg m_F$

$$E_p = k + \frac{m_F^2}{k} - \frac{m_F^4}{2k^3} \ln \frac{2k^2}{m_F^2} + \cdots , \qquad E_h = k + 2k \exp(-1 - 2k^2/m_F^2) + \cdots . \tag{21}$$

The most remarkable property of hole dispersion relation is that its minimum occurs at the nonzero momentum $k_* \simeq 0.4\, m_F$. The residues of the particle and hole propagators are given by [14]

Despite these subtleties, since $Z_p + Z_h \approx 1$ the fermionic dispersion relation can be well approximated by $\omega = [|\vec{k}|^2 + m_F^2(T)]^{1/2}$ (see fig. 1) and this is the form we have used in our calculation, verifying that it is accurate enough when its validity seems doubtful. Notice that temperature-dependent masses enter into the kinematics and into the dispersion relations, but spinor functions must be taken identical to vacuum spinors, although with a modified dispersion relation [14].

As for the bosonic case, we are interested only in the (11) component of the resummed fermionic propagator

$$S^{11}(K) = \cos^2\phi_K\,\Delta_F(K) - \sin^2\phi_K\,\Delta_F^*(K), \tag{22}$$

$$\Delta_F(K) = i\frac{(1+a)\gamma^\mu K_\mu + b\gamma^\mu U_\mu}{(1+a)^2K^2 + 2(1+a)bK\cdot U + b^2 + i\epsilon}. \tag{23}$$

Assuming that the self-energy Σ is real (which is always true in the high-T limit), so that a and b are real, with the help of eq. (9), we can rewrite eq. (22) as

$$S^{11}(K) = \left[(1+a)\gamma^\mu K_\mu + b\gamma^\mu U_\mu\right]\left[\frac{i}{[(1+a)\omega+b]^2 - (1+a)^2k^2 + i\epsilon}\right.$$
$$\left. -2\pi f_F(\omega)\delta\left([(1+a)\omega+b]^2 - (1+a)^2k^2\right)\right]. \tag{24}$$

Before applying these results to the computation of the baryon asymmetry, let us briefly discuss the issue of infrared singularities at finite temperature [15]. It is well-known that perturbation theory at finite temperature is afflicted by infrared problems which are worse than the ones appearing at zero-temperature field theory where the Kinoshita-Lee-Nauenberg (KLN) theorem [16, 17] demonstrates that singularities appearing at intermediate stages of the calculation cancel out in the final physical result. In an interacting scalar theory the plasma mass may receive large two-loop infrared contributions and an all-loop resummation is needed to get a final result. In this case the plasma mass obtained at one-loop is used as an infrared regulator. In order to deal with infrared divergences one can perform the so-called *hard thermal loop* (HTL) resummation [18]. In the HTL resummation one makes a distinction between hard momenta of order T and soft momenta of order gT and performs a resummation only for the soft lines. Indeed, the corrections to the bare propagator K^2, being of order g^2T^2, start to be relevant only when $K \sim gT$, which is the soft scale. Therefore, if the internal momentum is hard, then ordinary bare propagators and vertices are sufficient, but if the momentum is soft then effective propagators and vertices must be used. In this way, one obtains an improved perturbation theory, in which the HTLs become generic analytic functions of the external momenta, $g^nT^2f(\omega_i, k_i)$. Using the HTL technique, we have for instance explicitly checked that the top Yukawa coupling constant λ_t entering the vertex HQ_3U_3 (which is involved in the $\Delta L = 1$ scattering $LH \to Q_3U_3$) gets renormalized at finite temperature by the exchange of gauge bosons between the Higgs and the top lines and that the correction is tiny, $\delta\lambda_t/\lambda_t \simeq 10^{-1}\,g_2$. Furthermore one can extend the KLN theorem at finite temperature, and the infrared divergences in the corrections from virtual gauge-boson exchange cancel once we include absorption and emission of real particles that are too soft to escape the thermal bath [19].

3 Including thermal corrections

Performing a complete study of leptogenesis including all finite-temperature corrections is a very difficult task. In our computation we include the leading finite-temperature corrections

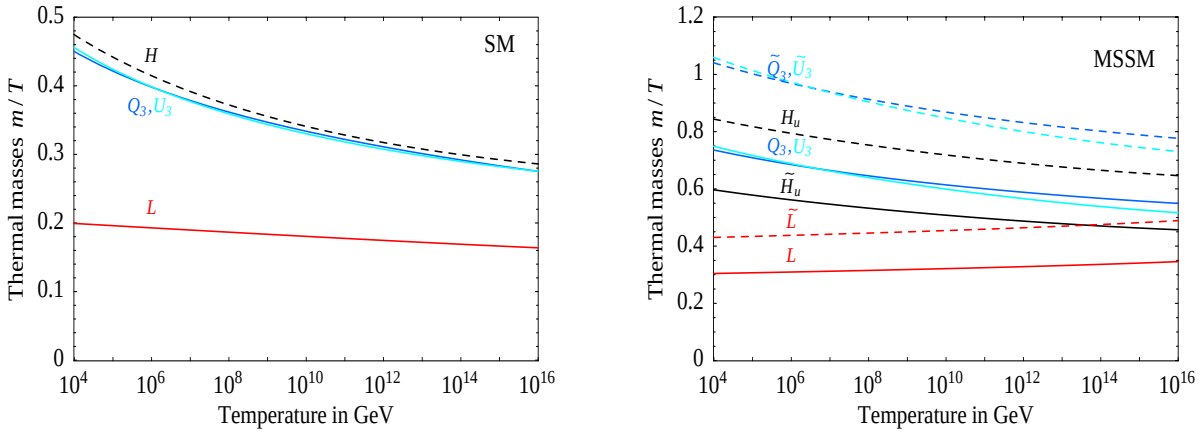

Figure 2: *Thermal masses in the SM (left) and in the MSSM (right), in units of the temperature T.*

which are quantitatively relevant for the computation of the final baryon asymmetry. These are given by: *i)* thermal corrections to gauge and Yukawa couplings; *ii)* thermal corrections to lepton, quark, and Higgs propagators; *iii)* thermal corrections to the CP-violating asymmetry.

In this section we discuss how we implement these three kinds of corrections and how large they are. Explicit formulæ can be found in the appendices. In the next section we indicate how the finite-temperature computation of the baryon asymmetry can be significantly simplified by including only those effects which a posteriori turn out to be numerically most relevant.

3.1 Corrections to couplings

Renormalization of gauge and Yukawa couplings in the thermal plasma has been extensively studied (see *e.g.* ref. [20]). A very good approximation is to renormalize the couplings at the first Matsubara mode,

$$E_r = 2\pi T, \tag{25}$$

using the zero-temperature renormalization group equations (RGE). This result can be understood by recalling that the average particle energy in the thermal plasma is larger than the temperature, and so must be the renormalization scale. For our purposes, the important couplings are the gauge and top Yukawa, which we evaluate using the appropriate RGE at the scale in eq. (25). Therefore those couplings are always functions of temperature, even if not explicitly indicated.

Leptogenesis also depends on neutrino couplings and masses. The neutrino mass matrix can be renormalized from low energy (where it is measured) up to the high-energy scale relevant for leptogenesis using the well known RGE reported in appendix B. They are

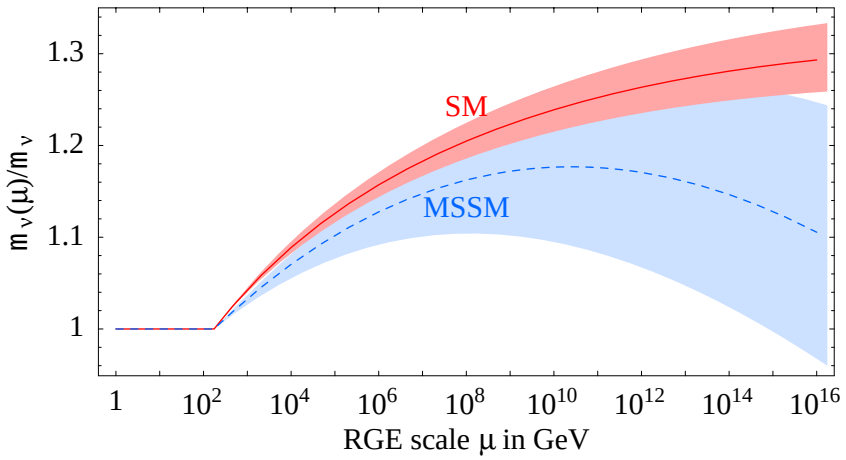

Figure 3: *Universal running of m_ν in the SM and in the MSSM. The bands give an indication of the uncertainties, as explained in the text.*

often solved with a 'diagonalize and run' approach which focuses on the neutrino masses and mixings probed by oscillation experiments. We instead purse a 'run and diagonalize' strategy, as *e.g.* in ref. [7], which makes it easier to see how the combinations of neutrino masses relevant for leptogenesis renormalize. The solution can be trivially written as $m(\bar{\mu}') = r\ I \cdot m(\bar{\mu}) \cdot I$ where r is an overall rescaling factor and

$$I \simeq \mathbb{1} + \mathrm{diag}(y_e^2, y_\mu^2, y_\tau^2)\frac{\ln(\bar{\mu}'/\bar{\mu})}{(4\pi)^2} \times \begin{cases} -3/2 & \text{in the SM} \\ 1/\cos^2\beta & \text{in the MSSM} \end{cases} \tag{26}$$

(higher powers of $\ln(\bar{\mu}'/\bar{\mu})$ can be easily resummed). Here $y_\ell = m_\ell/v$ with $v = 174\,\mathrm{GeV}$. Unless one considers large values of $\tan\beta$ the flavour dependent term I is very close to the unity matrix. In such a case, I can be relevant only if one considers special neutrino mass matrices, fine-tuned such that 2 or 3 eigenvalues are almost degenerate. We can neglect I, as long as we do not consider such cases.

The relevant correction to neutrino masses is therefore given by the overall rescaling factor r. Its numerical value is plotted in fig. 3. The SM value has been computed assuming $\alpha_3(M_Z) = 0.118 \pm 0.003$, a pole top mass of $m_t = 175 \pm 5\,\mathrm{GeV}$ and a Higgs mass $m_h = 115\,\mathrm{GeV}$. The band indicates the present uncertainty induced by the errors on m_t and α_3. Varying the Higgs mass has a negligible impact, unless m_h is close to the triviality bound, $m_h \sim 180\,\mathrm{GeV}$, where the quartic Higgs coupling becomes non-perturbative at high scales inducing arbitrarily large values of r.

The MSSM central value has been computed assuming also moderately large $\tan\beta \sim 10$, unification of gauge couplings at $M_{\mathrm{GUT}} = 2 \times 10^{16}\,\mathrm{GeV}$, and $\lambda_t(M_{\mathrm{GUT}}) = 0.6$. Ref. [21] explains why $\lambda_t(M_{\mathrm{GUT}})$ is still significantly uncertain, about between $0.5 \div 0.7$, giving rise to a correspondingly large uncertainty in RGE effects, illustrated by the shaded area in fig. 3.

3.2 Thermal corrections to decay and scattering processes

To calculate the generated baryon asymmetry of the universe in the thermal leptogenesis scenario we have to solve a set of Boltzmann equations, discussed in appendix A, which take into account processes that create or wash-out the asymmetry. We have recalculated the relevant reaction densities taking into account the propagation of particles inside the thermal plasma.

As discussed in section 2, the wave-functions that describe external fermion states in decay and scattering amplitudes are the same as in the zero-temperature case [14]. Temperature corrections appear only in internal fermion lines and in the kinematics. In the SM, for all processes except those involving gauge bosons (which will be discussed later), the only fermion which mediates an interaction relevant for leptogenesis is N_1. Since N_1 has no gauge interactions and its Yukawa coupling is small in all the relevant region of parameters, thermal corrections to N_1 propagation can be neglected[2].

Therefore we only have to include thermal corrections to the dispersion relations of lepton doublets, third-generation quarks and Higgs bosons (and their supersymmetric partners). Fig. 1a shows the dispersion relation $\omega(k)$ satisfied by a fermion with thermal mass m at temperature T. For simplicity, we approximate it with a Lorentz-invariant relation $\omega^2 = m^2 + k^2$, shown by the solid line in fig. 1a. As discussed later, this approximation has a negligible impact on our results.

Temperature corrections to the SM and MSSM particle masses are well known [22]. The relevant formulæ are collected in appendix B and the numerical values of m/T are plotted in fig. 2 as function of the temperature (assuming a Higgs mass $m_h = 115\,\mathrm{GeV}$). The computation of thermally corrected SM decay rates and reduced cross sections is performed in appendix B. Here we wish to discuss the most important features of the results.

The processes that affect SM thermal leptogenesis are (Feynman diagrams are plotted in fig. 4)

- the decays $N \to HL$ and (at very high temperature when the Higgs becomes heavier than N_1) $H \to NL$ (the relative reaction density is denoted as γ_D, see appendix B);
- the $\Delta L = 2$ scatterings $LH \to \bar{L}\bar{H}$ and $LL \to \bar{H}\bar{H}$ (γ_N);
- the $\Delta L = 1$ scatterings involving the top quark $N_1\bar{L} \to Q_3U_3$ (γ_{Ss}) and $LQ_3 \to N_1U_3$, $LU_3 \to N_1Q_3$ (γ_{St}) as well as their inverse reactions (which have the same reaction densities, up to small CP-violating corrections). We introduce $\Delta L = 1$ scatterings involving $\mathrm{SU}(2) \otimes \mathrm{U}(1)$ gauge bosons A: $N_1\bar{L} \to HA$ (γ_{As}), $LH \to N_1A$, $\bar{L}A \to N_1H$ (γ_{At}) and define the total scattering rates $\gamma_{Ss,t} = \gamma_{Hs,t} + \gamma_{As,t}$.

Fig. 5a shows the reaction densities γ_D, γ_{Ss}, γ_{St}, $4\gamma_N$, all normalized in units of Hn_{N_1}, as function of the temperature and for $\tilde{m}_1 = r \cdot |\Delta m^2_{\mathrm{atm}}|^{1/2} = 0.06$ eV and $m_{N_1} = 10^{10}\,\mathrm{GeV}$.

Fig. 5b (c) show the full set of reaction densities computed including (not including) the effects added in this paper. In these figures we use conventions adopted in previous

[2]We do not consider the case of quasi-degenerate right-handed neutrinos. In such a case small corrections which break degeneracy could not be neglected.

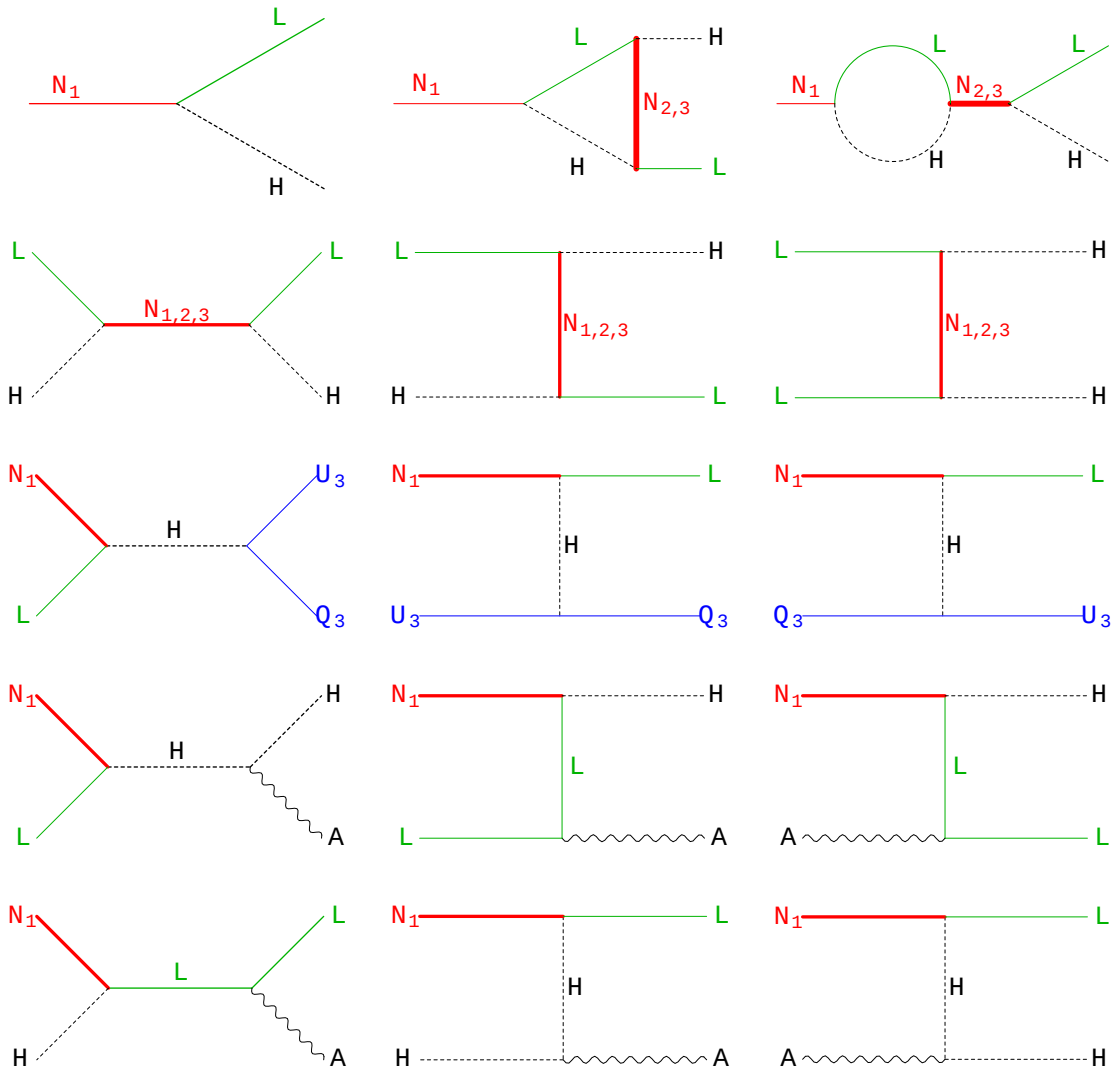

Figure 4: *Feynman diagrams contributing to SM thermal leptogenesis.*

papers, and plot γ_D, γ_{Hs}, γ_{Ht}, γ_{As}, γ_{At} normalized in units of Hn_{N_1} and the 'subtracted $\Delta L = 2$ scattering rate' (see appendix A) $\gamma_N^{\rm sub}$ normalized in units of Hn_γ.

Decays

The modification in γ_D is probably the most apparent feature of a comparison between fig. 5b and 5c, and it occurs because at sufficiently high temperature, the Higgs becomes heavier than N_1 and the decay $N_1 \to HL$ becomes kinematically forbidden. For temperatures in the range where $m_H - m_L < m_{N_1} < m_H + m_L$, there are no two-body decays involving N_1 at all. At higher temperatures the Higgs becomes heavy enough for

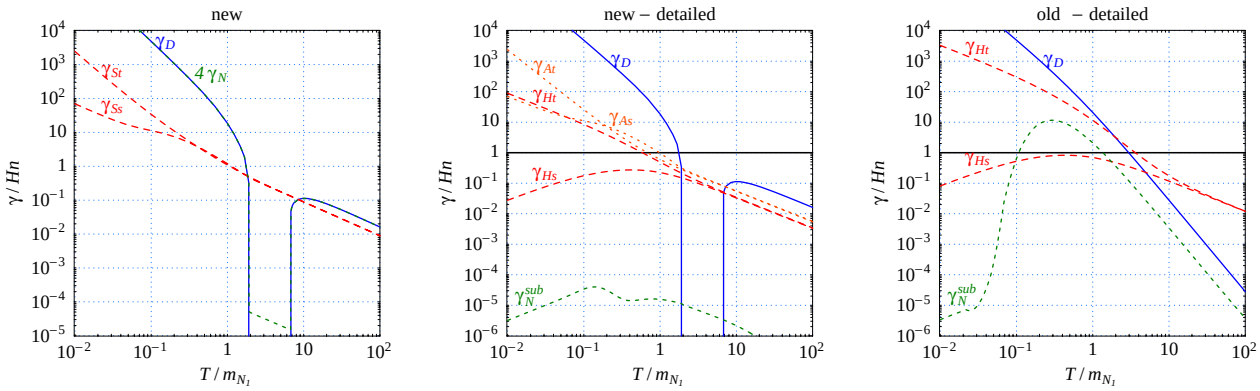

Figure 5: **The SM reaction densities** *for* $\tilde{m}_1 \equiv (Y_\nu Y_\nu^\dagger)_{11} v^2/m_{N_1} = 0.06\,\text{eV}$ *and* $m_{N_1} = 10^{10}\,\text{GeV}$. *Blue line: decays* ($\gamma_D$). *Red long-dashed lines:* $\Delta L = 1$ *scatterings* ($\gamma_{Ss,t} = \gamma_{Hs,t} + \gamma_{As,t}$). *Green dashed lines:* $\Delta L = 2$ *scatterings* (γ_N).

the $H \to N_1 L$ decays to be allowed, and the heavy neutrinos are produced in the process $H \leftrightarrow N_1 L$ rather than in $N_1 \leftrightarrow HL$. Including thermal masses we get $\gamma_D \propto T^4$ at $T \gg m_{N_1}$. Neglecting thermal masses gave a much smaller decay rate, $\gamma_D \propto T^2$, so that higher order $\Delta L = 1$ scatterings $\gamma_{Hs,t}$ were dominant.

$\Delta L = 1$ scatterings

A comparison of fig. 5b,c reveals other important numerical differences. There is a significant reduction of $\Delta L = 1$ scattering rates (red dashed curves), mainly γ_{H_t}, over the full temperature range. This comes from two different effects: 1) the top Yukawa coupling at high temperatures is smaller than at the electroweak scale, *e.g.* $y_t(10^{10}\,\text{GeV})/y_t(m_t) \approx 0.6$; 2) Higgs boson exchange in the t channel mediates a long-range force, giving rise to cross section enhanced by $\ln m_{N_1}/m_H$. This enhancement disappears when the thermal Higgs mass, $m_H \sim 0.4\,T$, is used in place of the zero-temperature Higgs mass, $m_H \sim 100\,\text{GeV}$. Such reduction of the $\Delta L = 1$ scattering rates turns out to be the most important modification and affects leptogenesis in two different ways: less washout of the leptonic asymmetry at $T \ll m_{N_1}$ and slower thermalization of N_1 at $T \gg m_{N_1}$. It is partially compensated by the inclusion of $\Delta L = 1$ scatterings involving gauge bosons.

$\Delta L = 2$ scatterings

There is a new resonant enhancement of $\Delta L = 2$ scatterings $LH \leftrightarrow \bar{L}\bar{H}$ mediated by N_1.[3] At low temperatures the virtual N_1 can be on-shell when exchanged in the s-channel, so that γ_N is enhanced by the s-channel resonance at $s = m_{N_1}^2$. At high temperatures the virtual N_1 can be on-shell when exchanged in the u-channel, so that γ_N is enhanced by the

[3]Scatterings mediated by the heavier $N_{2,3}$ are included as described in section 4.

u-channel resonance at $u = m_{N_1}^2$. For intermediate temperatures there is no resonance.

The s-channel resonance is regulated, as usual, by the N_1 width. On the contrary the new u-channel resonance occurs when N_1 is stable, because its decays are forbidden by thermal masses. The divergence in the cross section is eliminated by the presence of an imaginary part in the N_1 propagator, corresponding to the thermal damping rate caused by the interactions with the plasma. Although this effect depends in a complicated way on N_1 thermal motion with respect to the plasma, in narrow width approximation (i.e. for small N_1 Yukawa couplings) resonant enhancements give $\gamma_N \simeq \gamma_D/4$ (see appendix B).

Therefore we performed a precise computation of the decay rate (including also Pauli-blocking and stimulated emission factors, as discussed in appendix B) and computed $\gamma_N^{\rm sub} = \gamma_N - \gamma_D/4$, the contribution to the $\Delta L = 2$ scattering rate due only to off-shell scatterings. Indeed, this quantity enters the Boltzmann equations, because the contribution of on-shell N_1 exchange is already taken into account by successive decays and inverse decay processes, $LH \leftrightarrow N_1 \leftrightarrow \bar{L}\bar{H}$, and has to be subtracted in order to avoid double counting. In appendix A we show how to properly perform the subtractions to the N_1 propagator. Our result differs from the one of ref. [6, 9]. Indeed, the subtraction method used in ref. [6, 9] leaves a spurious contribution which effectively double counts the decay process. This is why our $\gamma_N^{\rm sub}$ in fig. 5b no longer has the "off-shell resonance" found by previous computations, shown in fig. 5c. At leading order in the neutrino Yukawa coupling Y_ν $\gamma_D, \gamma_{Ss}, \gamma_{St} \propto (Y_\nu Y_\nu^\dagger)_{11}$ and $\gamma_N^{\rm sub} \propto (Y_\nu Y_\nu^\dagger)_{11}^2$. Therefore, we find that the off-shell contribution is relevant only when $Y_\nu \sim 1$, which is not the case in our example of fig. 5. When $Y_\nu \sim 1$ a fully precise computation should include also $\Delta L = 0$ $L\bar{L} \to N_1 N_1$ scatterings, which would play a minor role, affecting the N_1 abundancy. More importantly, in such a case off-shell $\Delta L = 2$ scatterings suppress n_B exponentially, because (unlike $\Delta L = 2$ mediated by on-shell N_1) at $T \lesssim m_{N_1}$ they are not suppressed by the N_1 abundancy.

Furthermore, fig. 5b allows to get the rates for other values of $\tilde{m}_1$ by applying the appropriate rescaling. For other values of m_{N_1} the rescaling of the Yukawa couplings $(Y_\nu Y_\nu^\dagger)_{11} = \tilde{m}_1 m_{N_1}/v^2$ is the dominant effect, but is not the only one. One needs to recompute the rates taking into account the running of the couplings.

3.3 CP violation at finite temperature

In this section we investigate the finite-temperature effects on the CP asymmetries

$$\epsilon_i = \frac{\gamma^{\rm eq}(i \to f) - \gamma^{\rm eq}(\bar{i} \to \bar{f})}{\gamma^{\rm eq}(i \to f) + \gamma^{\rm eq}(\bar{i} \to \bar{f})} \ . \tag{27}$$

where $\gamma^{\rm eq}$ are the thermally averaged decay rates. The decay processes relevant to our analysis are $N_1 \to LH$, which is allowed for $m_{N_1} > m_L(T) + m_H(T)$ and $H \to LN_1$, which is allowed at higher T, when $m_H(T) > m_L(T) + m_{N_1}$ and is CP-violating only because of purely finite-T effects.

The issue of CP-violating decays at finite T was already investigated in ref. [23], although neglecting thermal masses. As we will see, the effect of the masses is crucial, giving a non-trivial T dependence of the CP violation. The effect of thermal masses is taken into

account by using the one-loop finite temperature resummed propagators, and by using modified dispersion relations, as discussed in section 2.

We choose to work in the rest frame of the plasma, where $U_\mu = (1, 0, 0, 0)$. In this way the finite-T Feynman rules are simplified, while the kinematics is more complicated, since we have to consider decaying particles in motion. Although we have performed our calculation in the general case, neglecting the thermal motion of the decaying particles allows to write reasonably accurate analytical approximations. As already said, we approximate the complicated dispersion relation for fermions with $\omega^2 = k^2 + m_F^2$.

The CP asymmetries in the relevant decays come from interference between the tree-level decay amplitude with the one-loop contributions. There are two relevant one-loop diagrams: the so-called vertex and wave-function contributions (shown in fig. 16). We compute the imaginary part of the one-loop graphs using the Cutkosky cutting rules at finite temperature [24], which are more complicated than at $T = 0$ (even in the absence of type-2 vertices). While at $T = 0$ most cuttings (in our case two of the three possible cuttings) give no contribution due to energy-conservation, this is no longer true at $T \neq 0$, since particles may absorb energy from the plasma. Formally, this means that we must also consider cut lines with negative-energy on-shell particles.

Nevertheless, we ignore cuts which involve heavy right-handed neutrinos $N_{2,3}$, because they are suppressed by a Boltzmann factor $\exp(-m_{N_{2,3}}/T)$, which is negligibly small since we assume a hierarchical spectrum $m_{N_{2,3}} \gg m_{N_1}$, and we work at T much smaller than $m_{N_{2,3}}$. Therefore, as illustrated in fig. 16 we can restrict ourselves to the standard cutting of the Higgs and lepton lines, but with energy flows in both directions.

CP-asymmetry in N_1 decay

We first consider the CP asymmetry in N_1 decay,

$$\epsilon_{N_1} \equiv \frac{\gamma^{\rm eq}(N_1 \to HL) - \gamma^{\rm eq}(N_1 \to \bar{H}\bar{L})}{\gamma^{\rm eq}(N_1 \to HL) + \gamma^{\rm eq}(N_1 \to \bar{H}\bar{L})}. \tag{28}$$

The full result employed in our leptogenesis code is presented in appendix C. Here we present a simple analytic approximation obtained neglecting the thermal motion of N_1 with respect to the plasma, which is justified at $T \ll m_{N_1}$ and still reasonably accurate at higher temperatures (see fig. 6a). The result is

$$\epsilon_{N_1}(T) = \epsilon_{N_1}(0) R_\epsilon(T)\,, \qquad \epsilon_{N_1}(0) = \frac{1}{8\pi} \sum_{j\neq 1} \frac{{\rm Im}\left[(Y^\dagger Y)^2_{j1}\right]}{\left[Y^\dagger Y\right]_{11}} f\left(\frac{m^2_{N_j}}{m^2_{N_1}}\right). \tag{29}$$

The function f describes the usual result at $T = 0$ which, in the SM, is given by

$$f(x) = \sqrt{x}\left[\frac{x-2}{x-1} - (1+x)\ln\left(\frac{1+x}{x}\right)\right] \stackrel{x\gg 1}{\longrightarrow} -\frac{3}{2\sqrt{x}}\,. \tag{30}$$

The thermal correction is described by the function R_ϵ, given by[4]

$$R_\epsilon = 16\frac{k^2}{m_{N_1}}[\omega(1+a_L)+b_L]J[1+f_H-f_L-2f_Hf_L] \qquad J = \left|\left|\begin{matrix}\partial\delta_H/\partial\omega & \partial\delta_L/\partial\omega \\ \partial\delta_H/\partial k & \partial\delta_L/\partial k\end{matrix}\right|\right|^{-1} \tag{31}$$

where $||M|| \equiv |\det M|$, $K_L = (\omega, k)$ is the energy-momentum quadri-vector of L, and the functions $a_L \equiv a(K_L)$ and $b_L \equiv b(K_L)$ are defined in eq.s (16,17). The Fermi-Dirac and Bose-Einstein distributions

$$f_L = (e^{E_L/T}+1)^{-1} \qquad f_H = (e^{E_H/T}-1)^{-1}$$

in the third factor are evaluated at the fermion energy $E_L = \omega$ and at the boson energy $E_H = m_{N_1} - \omega$. The first term is obtained by computing the relevant Feynman graph in the limit $m_{N_{2,3}} \gg m_{N_1}$ and dividing by the tree level rate. The Jacobian J is obtained when imposing the on-shell conditions for the cut particles H and L

$$\delta_H \equiv (m_{N_1}-\omega)^2 - k^2 - m_H^2 = 0 \qquad \delta_L \equiv [(1+a_L)\omega + b]^2 - (1+a_L)^2k^2 = 0 \tag{32}$$

which fixes the values of ω and k in terms of m_{N_1}, m_L, m_H. As discussed in section 2 the equation for L has two different solutions: 'particles' and 'holes'. A numerical computation shows that the 'hole' contribution to the CP-asymmetry is negligible because, as explained in section 2, relativistic holes have negligible interactions. The 'particle' contribution is well approximated by inserting in eq. (31) the values of ω and k

$$\omega = \frac{m_{N_1}^2 + m_L^2 - m_H^2}{2m_{N_1}}, \qquad k = \sqrt{\omega^2 - m_L^2} \tag{33}$$

obtained approximating $\delta_L \approx \omega^2 - k^2 - m_L^2 = 0$.

The main feature shown in fig. 6 is that $\epsilon(T)$ goes to zero as the temperature increases and the process becomes kinematically forbidden. This happens because the particles in the final state coincide with the cut particles in the loop: L and H. Therefore the threshold at which the cut particles can no longer be on the mass-shell is the same at which the decay becomes kinematically forbidden, i.e. when $m_{N_1} \approx m_H + m_L$.

There is another important effect which gives an additional suppression. The $1 + f_B - f_F - 2f_Bf_F$ factor in eq. (31) was first derived by the authors of ref. [23] who, neglecting the L and H thermal masses and thus setting $\omega = m_{N_1}/2$, found it to be equal to 1. However, only if the arguments of the Bose-Einstein and Fermi-Dirac distributions are the same, there is a peculiar cancellation: $f_B - f_F - 2f_Bf_F = 0$. Physically this cancellation can be understood as a compensation between stimulated emission and Pauli blocking. Only if bosons and fermions enter with the same energy, an exact cancellation holds.

[4]If $N_{2,3}$ are not much heavier than N_1 one can easily include effects suppressed by higher powers of $m_{N_1}/m_{N_{2,3}}$, obtaining a more lengthy analytical expression.

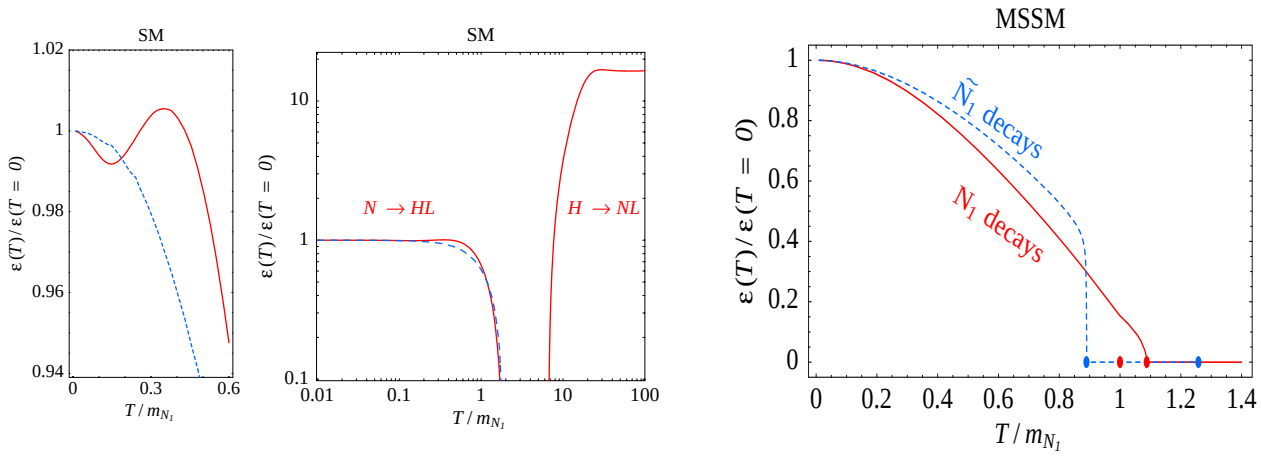

Figure 6: **Thermal corrections to the CP asymmetry**. $\epsilon(T)/\epsilon(T=0)$ *as a function of temperature for* $m_{N_{2,3}} \gg m_{N_1} = 10^{10}\,\mathrm{GeV}$ *in the SM (left plots) and in the MSSM (right plot, the dots indicate the various thresholds for* N_1 *and* $\tilde{N}_1$ *decays). In the SM plot the solid line shows our more accurate result derived in appendix C, while the dashed line shows the approximate result described in the main text, obtained neglecting the* N_1 *thermal motion.*

CP-asymmetry in H decay

The computation of the CP asymmetry in Higgs decay,

$$\epsilon_H \equiv \frac{\gamma^{\rm eq}(H \to N_1 L) - \gamma^{\rm eq}(\bar{H} \to N_1 \bar{L})}{\gamma^{\rm eq}(H \to N_1 L) + \gamma^{\rm eq}(\bar{H} \to N_1 \bar{L})}, \tag{34}$$

is similar to the previous one, although with some important differences. Also in this case there are two relevant cuts (in wave and vertex one loop diagrams, see fig. 17) which involve the Higgs and lepton lines. The difference is that such graphs would have no imaginary parts with the usual Feynman rules at $T = 0$, as cuttings of H and L would be kinematically forbidden. On the contrary, at finite T absorption of particles by the plasma allows also negative energies in the cuts. The asymmetry ϵ_H turns out to be proportional to the purely thermal factor $f_H - f_L - 2f_H f_L$. The non-standard cut (see fig. 17) implies a more complicated kinematics which does not allow us to obtain an analytic result for ϵ_H. The computation is presented in appendix C, where we neglect effects due to particle motion and due to non-trivial fermion dispersion relation, since eventually ϵ_H turns out to have a negligible effect on the final results for leptogenesis. ϵ_H approaches a constant value at high $T \gg m_{N_1}$ (see fig. 6).

CP-asymmetries in the MSSM

The situation in the MSSM becomes more complicated than in the SM because we must now study both N_1 and $\tilde{N}_1$ decays, each having two possible decay channels, with each channel having more diagrams. The CP-asymmetries at zero temperature were first computed correctly in ref. [25]. We do not study H and $\tilde{H}$ decays, which appear only at high temperature.

The computations at finite temperature are analogous to the SM case and described in appendix D. The result is different because the cut particles in the loop are different from the final-state particles: the threshold at which the cut particles can no more go on-shell is different from the one at which the decay becomes forbidden. Therefore, in the single decay modes, CP-violation disappears either before or after the decay mode becomes kinematically forbidden.

The source of CP-asymmetry which appears in the MSSM Boltzmann equations are the CP-asymmetries ϵ_{N_1} and $\epsilon_{\tilde{N}_1}$ in N_1 and $\tilde{N}_1$ decays, averaged over the different decay channels $N_1 \to HL, \tilde{H}\tilde{L}$ and $\tilde{N}_1 \to H\tilde{L}, \tilde{H}L$. As illustrated in fig. 6b ϵ_{N_1} and $\epsilon_{\tilde{N}_1}$ behave in rather different ways.

Like in the SM, ϵ_{N_1} goes to zero at the same temperature threshold at which N_1 decays become kinematically forbidden, as a consequence of the fact that both decay channels contribute to the imaginary part of both decay modes.

On the contrary, for $\epsilon_{\tilde{N}_1}$, only one-loop diagrams with internal bosons $H, \tilde{L}$ contribute to the CP-asymmetry of decays into fermions $\tilde{H}, L$ and viceversa: since thermal corrections make bosons heavier than the corresponding fermions (see appendix B) $\epsilon_{\tilde{N}_1}$ vanishes when $\tilde{N}_1$ decays into fermions are still kinematically allowed. The dashed line in fig. 6b shows the final result. Thermal corrections are significant at $T \sim m_{N_1}$, but give almost no effect at lower temperatures. This happens in a non-trivial way. Decays into scalars have a rate significantly enhanced by stimulated emission and a CP-asymmetry significantly suppressed by Pauli blocking, while the opposite happens for decays into fermions. If thermal masses can be neglected, the two effects compensate each other, as noticed in ref. [23]. This cancellation no longer takes place when thermal masses become sizable, giving rise to the behavior of $\epsilon_{\tilde{N}_1}(T)$ shown in fig. 6b.

4 Leptogenesis in the Standard Model

We assume that right-handed neutrinos are hierarchical, $m_{N_{2,3}} \gg m_{N_1}$ so that we have to study the evolution of the number density of N_1 only. In such a case the final amount of $\mathcal{B}-\mathcal{L}$ asymmetry $Y_{\mathcal{B}-\mathcal{L}} = n_{\mathcal{B}-\mathcal{L}}/s$ generated by N_1 assuming no pre-existing asymmetry can be conveniently parameterized as

$$Y_{\mathcal{B}-\mathcal{L}} = -\epsilon_{N_1}\, \eta\, Y_{N_1}^{\rm eq}(T \gg m_{N_1}). \tag{35}$$

Here ϵ_{N_1} is the CP-asymmetry parameter in N_1 decays *at zero temperature*, and $Y_{N_1}^{\rm eq}(T \gg m_{N_1}) = 135\zeta(3)/(4\pi^4 g_*)$, where g_* counts the effective number of spin-degrees of freedom in thermal equilibrium ($g_* = 106.75$ in the SM with no right-handed neutrinos)[5]. η is an efficiency factor that measures the number density of N_1 with respect to the equilibrium

[5]The formula used in our numerical code includes leading order thermal effects from quarks, leptons and gauge bosons (neglecting Yukawa couplings):

$$\rho = \rho_R + \rho_{N_1}, \qquad \rho_R = \left[\frac{427}{4}\frac{\pi^2}{30} - \frac{7}{4}g_3^2 - \frac{19}{32}g_2^2 - \frac{25}{96}g_Y^2\right]T^4 \qquad s = \frac{4\rho_R}{3T}.$$

value, the out-of-equilibrium condition at decay, and the thermal corrections to ϵ_{N_1}. Recalling that, after reprocessing by sphaleron transitions, the baryon asymmetry is related to the $\mathcal{B}-\mathcal{L}$ asymmetry by

$$\frac{n_{\mathcal{B}}}{s} = \frac{24+4n_H}{66+13n_H}\frac{n_{\mathcal{B}-\mathcal{L}}}{s}, \tag{36}$$

where n_H is the number of Higgs doublets, for the SM we find

$$\frac{n_{\mathcal{B}}}{s} = -1.38\times 10^{-3}\epsilon_{N_1}\eta. \tag{37}$$

Assuming the 'standard' ΛCDM cosmological model, BBN and WMAP measurements imply

$$\frac{n_{\mathcal{B}}}{n_\gamma} = (6.15\pm 0.25)\times 10^{-10} \qquad \text{with} \qquad s = 7.04\ n_\gamma. \tag{38}$$

Computing η is the most difficult part of the calculation, since it is obtained from numerical solution of Boltzmann equations. In general the result depends on how the lepton asymmetry is distributed in the three lepton flavours. For simplicity one usually ignores flavour issues and solves the approximated Boltzmann equation for the total lepton asymmetry described in appendix A. If all mixing angles of left and right-handed neutrinos are large, as data might suggest, this 'one-flavour approximation' is accurate up to $\mathcal{O}(1)$ corrections. In order to include flavour factors one must solve the Boltzmann equations for the 3×3 density matrix of lepton doublets, as discussed in ref. [26].

The $\Delta L=2$ scatterings mediated by heavier right-handed neutrinos $m_{N_{2,3}} \gg m_{N_1}$ are relevant at $m_{N_1}\gtrsim 10^{14}\,\text{GeV}$. Below, they can have $\mathcal{O}(1)$ effects if neutrinos are quasi-degenerate. Although these scatterings are produced by the same effective dimension 5 operator that generates neutrino masses, their contribution to $\hat{\sigma}_{Ns,t}$ depends on unknown high-energy parameters: the flavour composition of the neutrino coupled to N_1. Therefore, following ref. [26], we introduce a parameter ξ that, in eqs. 76–77, parameterizes the unknown contribution of $N_{2,3}$, which is important only if $m_{N_1}\gtrsim 10^{14}\,\text{GeV}$. If there were only one neutrino flavour with mass m_ν, the value of ξ would be $\xi = m_\nu/\tilde{m}_1 - 1$. With three neutrinos we cannot even write the precise definition of ξ, as flavour factors cannot be correctly included in Boltzmann equations valid in 'one-flavour approximation'. In our numerical results we assumed $\xi = \max(1, m_{\text{atm}}/\tilde{m}_1)$: if all mixing angles are large this choice is reasonably correct in all the parameter space.

Having fixed ξ, in 'one-flavour approximation' η depends only on two parameters:

$$\tilde{m}_1 \equiv (Y_\nu Y_\nu^\dagger)_{11} v^2/m_{N_1} \qquad \text{and} \qquad m_{N_1}$$

(and almost only on $\tilde{m}_1$ if $m_{N_1}\ll 10^{14}\,\text{GeV}$ i.e. when $\Delta L=2$ scatterings mediated by N_i off-resonance are negligible). This well-known fact remains true also when thermal corrections are included, as can be seen from appendix B. The parameter $\tilde{m}_1$ is 'the contribution to the neutrino mass mediated by N_1'. To see what this means in practice, let us temporarily assume that the left-handed neutrinos have a hierarchical spectrum

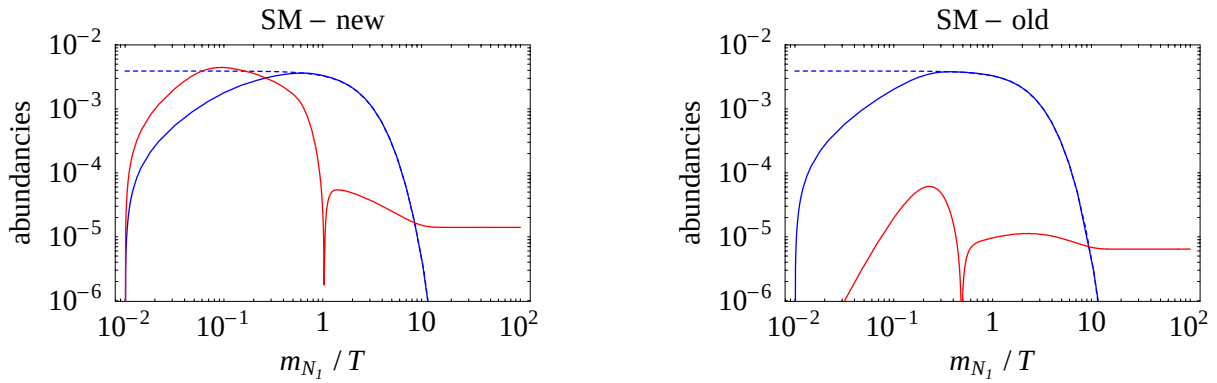

Figure 7: *Evolution of Y_{N_1} (blue curves) and $|Y_{B-L}/\epsilon_{N_1}|$ (red curves) with temperature in the SM. We fix $m_{N_1} = 10^{10}$ GeV and $\tilde{m}_1(m_{N_1}) = 0.06\,\mathrm{eV}$. The dashed line shows the thermal abundance of Y_{N_1}. Left plot: full computation, the efficiency is $\eta = 0.0036$. Right plot: no new effect included (and on-shell scatterings incorrectly subtracted), $\eta = 0.0017$.*

$m_1 \ll m_2 = m_{\rm sun} \ll m_3 = m_{\rm atm} \equiv |\Delta m^2_{\rm atm}|^{1/2}$. In such a case $\tilde{m}_1 = m_{\rm atm}$ if N_1 exchange gives rise to the atmospheric mass splitting, or $\tilde{m}_1 \gtrsim m_{\rm sun}$ if N_1 gives rise to the solar mass splitting. A smaller $\tilde{m}_1 \geq m_1$ can be obtained if N_1 gives rise to m_1, which can be arbitrarily small. A $\tilde{m}_1$ larger than $m_{\rm atm}$ can be obtained if $N_{2,3}$ exchange cancels out the N_1 contribution to neutrino masses. Stronger (weaker) restrictions are obtained if there are less (more) than 3 right-handed neutrinos.

In conclusion, measuring neutrino masses does not fix $\tilde{m}_1$ and m_{N_1}, which remain as free parameters. Therefore we compute η as function of m_{N_1} and of $\tilde{m}_1$ renormalized at the high scale m_{N_1} (at high scales $\tilde{m}_1$ is about $(20 \div 30)\%$ larger than at low energy).

Results

Figure 7 shows the evolution of the N_1 and $\mathcal{B}-\mathcal{L}$ abundances at our sample 'atmospheric' point: $\tilde{m}_1(m_{N_1}) = r(\Delta m^2_{\rm atm})^{1/2} = 0.06\,\mathrm{eV}$ and $m_{N_1} = 10^{10}\,\mathrm{GeV}$. For these values the N_1 abundancy remains close to thermal equilibrium, so that leptogenesis is mainly determined only by the later stages of the evolution at relatively small temperatures. This explains why, despite the significant variations at higher temperature, there is only a mild correction to the final baryon asymmetry. Proper subtraction of on-shell scatterings reduces wash-out by a 3/2 factor. This gives a 3/2 increase of the efficiency, as can be seen from the analytical approximation of ref. [26].

We now present our results for the thermal leptogenesis efficiency parameter η. We assume no pre-existing $\mathcal{B}-\mathcal{L}$ asymmetry, and we study the three cases of

(0) zero initial N_1 population, $Y_{N_1} = 0$ at $T \gg m_{N_1}$. This case can be realized *e.g.* if an inflaton field reheated the universe decaying mostly into SM particles.

(1) thermal initial N_1 population, $Y_{N_1} = Y^{\rm eq}_{N_1}$ at $T \gg m_{N_1}$. This case can be realized in

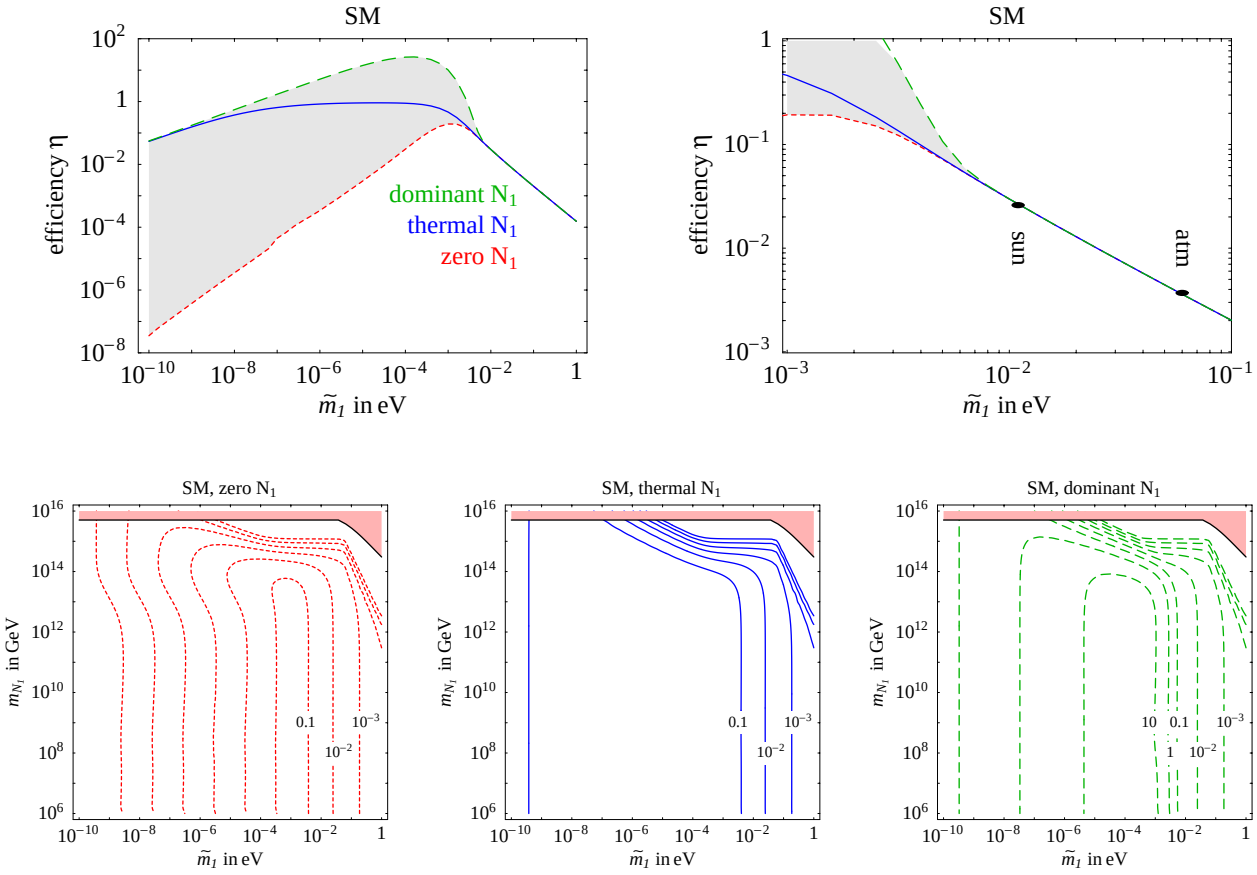

Figure 8: **Efficiency η of leptogenesis** *in the SM, assuming zero (dashed red line), thermal (continuous blue line) or dominant (long dashed green line) initial N_1 abundancy. Upper plots: η as function of $\tilde{m}_1$ (renormalized at m_{N_1}) for $m_{N_1} = 10^{10}\,\mathrm{GeV}$. Lower plots: contours of $\eta(\tilde{m}_1, m_{N_1}) = 10^{-6,-5,\ldots,0,1}$. In the shaded regions the neutrino Yukawa couplings are non-perturbative.*

presence of extra interactions at $T \gg m_{N_1}$, mediated *e.g.* by a heavy Z' boson related to SO(10) unification.

(∞) dominant initial N_1 abundancy, $\rho_{N_1} \gg \rho_R$ at early times. This case can be realized *e.g.* if an inflaton field reheated the universe decaying mostly into N_1.

In order to study the latter case we modified the Boltzmann equations employed in previous analyses including the effects of N_1 reheating (in the case (1) N_1 reheating is relevant only if $\tilde{m}_1 \lesssim 10^{-6}\,\mathrm{eV}$).

If $m_{N_1} \ll 10^{14}\,\mathrm{GeV}$ the efficiency parameter η depends almost only on $\tilde{m}_1$. In fig. 8 we show $|\eta|$ as function of $\tilde{m}_1$ for $m_{N_1} = 10^{10}\,\mathrm{GeV}$. If $\tilde{m}_1 > 10^{-2}\,\mathrm{eV}$ neutrino Yukawa couplings keep N_1 so close to thermal equilibrium that η does not depend on the unknown initial N_1 abundancy (similarly, an eventual pre-existing lepton asymmetry would be washed out if N_1 Yukawa couplings act on all flavours).

At smaller $\tilde{m}_1$ the efficiency η depends on the initial N_1 abundancy, ranging between the limiting cases (0) and (∞), as illustrated by the gray band in fig. 8. As expected, the maximal value of $\eta \sim g_*$ is reached at $\tilde{m}_1 \sim \tilde{m}_1^* \equiv 256\sqrt{g_*}v^2/3M_{\rm Pl} = 2.2 \times 10^{-3}\,{\rm eV}$ in case (∞). In such a case, η decreases at $\tilde{m}_1 \ll \tilde{m}_1^*$, because N_1 decays out-of-equilibrium at temperature $T_{\rm RH}^{N_1} \sim m_{N_1}\sqrt{\tilde{m}_1/\tilde{m}_1^*} \ll m_{N_1}$ so that N_1 reheating washes out some lepton asymmetry. In more physical terms, the particles H, L emitted in N_1 decays have energy larger than the temperature T, and split up in $\sim m_{N_1}/T_{\rm RH}^{N_1}$ particles without correspondingly increasing the lepton asymmetry, so that $\eta \sim g_*\sqrt{\tilde{m}_1^*/\tilde{m}_1}$.

When $\tilde{m}_1 \lesssim 10^{-6}\,{\rm eV}$, N_1 reheating starts to be significant even in case (1) giving $\eta < 1$. In fact, even if N_1 initially has a thermal abundancy $\rho_{N_1}/\rho_R \sim g_{N_1}/g_* \ll 1$, its contribution to the total density of the universe becomes no longer negligible, $\rho_{N_1}/\rho_R \sim (g_{N_1}m_{N_1})/(g_\star T)$, if it decays strongly out of equilibrium at $T \ll m_{N_1}$. For the reasons explained above, this effect gives a suppression of η (rather than an enhancement), and for very small $\tilde{m}_1$ the case (1) and (∞) give the same result.

The lower panel of fig. 8 contains our result for the efficiency $|\eta|$ of thermal leptogenesis computed in cases (0), (1) and (∞) as function of both $\tilde{m}_1$ and m_{N_1}. At $m_{N_1} \gtrsim 10^{14}\,{\rm GeV}$ non-resonant $\Delta L = 2$ scatterings enter in thermal equilibrium strongly suppressing η. Details depend on unknown flavour factors.

Our results in fig. 8 can be summarized with simple analytical fits

$$\frac{1}{\eta} \approx \frac{3.3 \times 10^{-3}\,{\rm eV}}{\tilde{m}_1} + \left(\frac{\tilde{m}_1}{0.55 \times 10^{-3}\,{\rm eV}}\right)^{1.16} \qquad \text{in case (0)} \tag{39}$$

valid for $m_{N_1} \ll 10^{14}\,{\rm GeV}$. This enables the reader to study leptogenesis in neutrino mass models without setting up and solving the complicated Boltzmann equations.

Implications

Experiments have not yet determined the mass m_3 of the heaviest mainly left-handed neutrino. We assume $m_3 = \max(\tilde{m}_1, m_{\rm atm})$. Slightly different plausible assumptions are possible when $\tilde{m}_1 \approx m_{\rm atm}$, and very different fine-tuned assumptions are always possible. As discussed above, we assume $\xi = m_3/\tilde{m}_1$ (the parameter ξ controls $\Delta L = 2$ scatterings mediated by $N_{2,3}$). These assumptions do not affect the absolute bounds on the masses of left-handed and right-handed neutrinos that we now discuss, but allow to present them in one simple plot, fig. 9.

The crucial assumption behind fig. 9 is that right-handed neutrinos are hierarchical. Under this hypothesis the CP asymmetry is bounded by [27, 9]

$$|\epsilon_{N_1}| \leq \frac{3}{16\pi}\frac{m_{N_1}m_3}{v^2}\left(1 - \frac{m_1}{m_3}\sqrt{1 + \frac{m_3^2 - m_1^2}{\tilde{m}_1^2}}\right) \tag{40}$$

where all parameters are renormalized at the high-energy scale $\sim m_{N_1}$ and $m_3^2 = m_1^2 +$

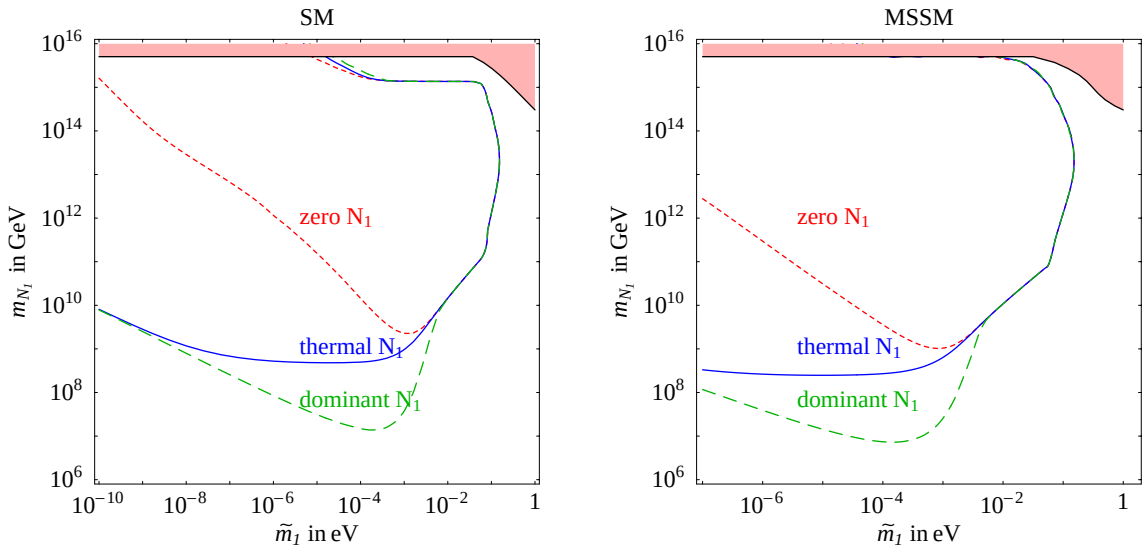

Figure 9: **Allowed range of $\tilde{m}_1$ and m_{N_1}** *for leptogenesis in the SM and MSSM assuming $m_3 = \max(\tilde{m}_1, m_{\rm atm})$ and $\xi = m_3/\tilde{m}_1$. Successful leptogenesis is possible in the area inside the curves (more likely around the border).*

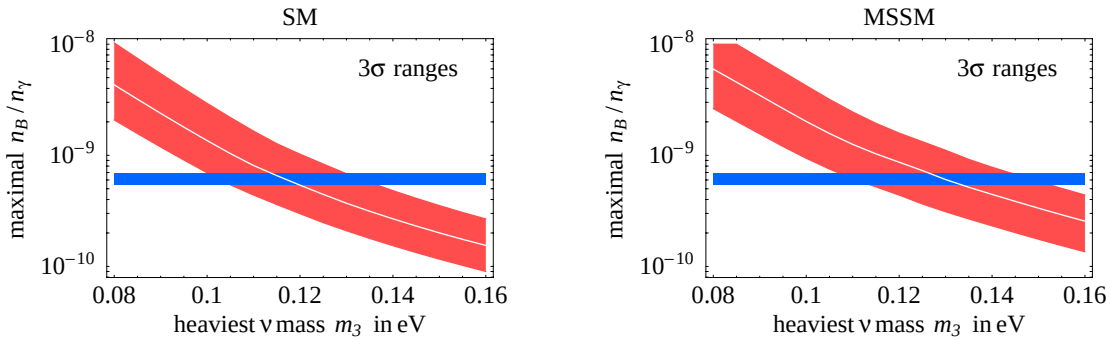

Figure 10: **Leptogenesis bound on neutrino masses**. *The plot shows the measured baryon asymmetry (horizontal line) compared with the maximal leptogenesis value as function of the heaviest neutrino mass m_3, renormalized at low energy. Error bars are at 3σ.*

$\Delta m^2_{\rm atm} + \Delta m^2_{\rm sun}$. The 3σ ranges of $m_{\rm atm}$ and of $n_{\mathcal{B}}/n_\gamma$ imply the lower bound

$$m_{N_1} > \frac{4.5 \times 10^8\,\text{GeV}}{\eta} > \begin{cases} 2.4 \times 10^9\,\text{GeV} & \text{in case (0)} \\ 4.9 \times 10^8\,\text{GeV} & \text{in case (1)} \\ 1.7 \times 10^7\,\text{GeV} & \text{in case } (\infty) \end{cases} \tag{41}$$

with the absolute bound realized in case (∞).

The allowed regions are shown in fig. 9 as function of $\tilde{m}_1$. The bound on m_{N_1} becomes stronger if left-handed neutrinos are heavier than what suggested by oscillations, $m_3 >$

$m_{\rm atm}$, until thermal leptogenesis can no longer generate the observed $n_{\mathcal{B}}$ (see fig. 9) giving an upper bound on the mass of degenerate neutrinos of about 0.1 eV [9]. This happens because η decreases with $\tilde{m}_1$ in the region of interest and, more importantly, because the bound in eq. (40) on ϵ_{N_1} for $m_3^2 - m_1^2 = m_{\rm atm}^2$ and $m_3 > m_{\rm atm}$ behaves as $1/m_3^3$.[6]

In order to study precisely the bound on neutrino masses we relax our simplifying assumptions on ξ and m_3 and compute the maximal baryon asymmetry generated by thermal leptogenesis as function of m_3. The results is shown in fig. 10: including the new effects discussed in this paper and combining errors on $\Delta m_{\rm atm}^2$ and on the baryon asymmetry in quadrature we get $m_\nu < 0.13\,\text{eV}$ at 99.73% CL (i.e. 3σ). The small difference with respect to previous results [9] is due to various factors: correct subtraction of on-shell scatterings (makes leptogenesis 50% more efficient and the bound on neutrino masses 7% weaker); renormalization of neutrino masses (makes the bound 7% stronger); renormalization of λ_t, inclusion of gauge scatterings, of thermal corrections, updated experimental determination of $\Delta m_{\rm atm}^2$ and of $n_{\mathcal{B}}/n_\gamma$.

We stress that the bound in eq. (40) on the CP-asymmetry holds because we assumed $m_{N_1} \ll m_{N_{2,3}}$: if right-handed neutrinos were instead quasi-degenerate CP violation in mixing can give an arbitrarily large CP-asymmetry, $\epsilon_{N_1} \sim 1$ and all bounds that we discussed evaporate. In particular the leptogenesis bound on the neutrino masses holds under the dubious assumption that hierarchical right-handed neutrinos give quasi-degenerate left-handed neutrinos.

4.1 Simple approximation

While in our calculations we use our full code, we now also discuss how the computation can be significantly simplified by including only the following new ingredients which, a posteriori, turn out to be numerically most relevant. Neglecting all these effects we reproduce the results in ref. [28]. Effects 2, 3, 4 were included in ref. [26]: neglecting the other ones we reproduce their results.

1 Proper subtraction of the on-shell N_1 propagators in $\Delta L = 2$ scattering processes, as discussed in Appendix A.

2 Neutrino masses have to be renormalized at the proper energy scale $\sim m_{N_1}$, both when computing η and ϵ_{N_1}.

Typically these effects give $\mathcal{O}(1)$ corrections. For $\tilde{m}_1 \gtrsim 10^{-3}$ eV the efficiency increases by up to almost a factor 2, due to the suppression of $\Delta L = 1$ wash-out processes caused by the following thermal effects:

3 Temperature corrections to the Higgs boson mass, $m_H \sim 0.4\,T$, must be included at least when computing the IR-enhanced $LN \to Q_3 U_3$ interaction rate.

[6] The bound on neutrino masses is saturated around $m_{N_1} \sim 10^{13}\,\text{GeV}$ and $\tilde{m}_1 \sim 0.1\,\text{eV}$. For these values computing leptogenesis in 'one flavour approximation' seems reliable. The Yukawa coupling of N_1 is ~ 0.3, and the couplings of $N_{2,3}$ are larger. Therefore one should worry that the bound on ϵ_{N_1} is obtained using its one-loop approximation, while two-loop effects can be important. Finally, we assume that the Higgs quartic coupling remains perturbative up to high energies.

4 The top Yukawa coupling must be renormalized at the proper energy scale $\sim m_{N_1}$.

These variations are partially compensated by

5 Inclusion of previously neglected scatterings involving weak gauge bosons A, $N_1 L \leftrightarrow HA$, $N_1 H \leftrightarrow LA$ and $N_1 A \leftrightarrow HL$. These extra scatterings are sizable because $g_2 > \lambda_t$ at energies above $10^9\,\mathrm{GeV}$: λ_t is no longer the dominant coupling. These processes have been recently considered for the time in ref. [29]

Including these contributions one gets an excellent approximation for $\tilde{m}_1 \gtrsim 10^{-3}\,\mathrm{eV}$. In order to get an approximation which is accurate also at $\tilde{m}_1 \ll 10^{-3}\,\mathrm{eV}$, in case (0) one needs to include one more effect:

6 Thermal corrections to the CP-violating parameter ϵ_{N_1}.

which turns out to have a sizable impact due to a more subtle reason.

Neglecting washout scatterings (which are small at $\tilde{m}_1 \ll 10^{-3}\,\mathrm{eV}$) and the temperature dependence of the CP asymmetry, in case (0) the Boltzmann equations are solved by $Y_{\mathcal{B}-\mathcal{L}} = +\epsilon_{N_1} Y_{N_1}$. In this approximation the lepton asymmetry generated in inverse-decay processes at $T \gg m_{N_1}$ when $Y_{N_1} < Y_{N_1}^{\mathrm{eq}}$ is exactly cancelled by the asymmetry generated later in N_1 decays when $Y_{N_1} > Y_{N_1}^{\mathrm{eq}}$. Consequently the effect which dominantly breaks this cancellation has a numerically important impact even if it is 'small'. 1) Washout interactions, dominated by γ_D, erase the lepton asymmetry generated at earlier stages more than the one generated at later stages, giving a small positive η. 2) Thermal corrections to ϵ slightly reduce it at small temperatures $T \sim m_{N_1}/4$, giving a small positive η.[7]

Finally, if one wants to study cases where N_1 can give a substantial contribution to the total energy density, one must include this correction in the Boltzmann equations, as described in appendix A.

5 Leptogenesis in the MSSM

In the case of the supersymmetric extension of the SM, the computation becomes more involved because of the presence of many new particle degrees of freedom. In particular, a lepton asymmetry is generated in decays of both the right handed neutrino N_1 and the right-handed sneutrino $\tilde{N}_1$. Since supersymmetry breaking can be ignored (except in special cases [10, 11]), the computation is somewhat simplified by the identities demanded by supersymmetry, such as $m_{N_1} = m_{\tilde{N}_1}$ and $\Gamma_{N_1} = \Gamma_{\tilde{N}_1}$. Thermal corrections break supersymmetry, so that it is rather ponderous to include them. At the moment, we do not attempt to make a full calculation in the supersymmetric case.

[7] The solid line in fig. 6a shows our most accurate result for thermal corrections to ϵ, that we employ in numerical computations. The enhancement at $T \sim 0.4 m_{N_1}$ comes from the quantum statistics factor, $1 + f_H - f_L - 2 f_H f_L$, that can be larger than one when both thermal masses and N_1 motion with respect to the plasma are taken into account. In case (0) for $\tilde{m}_1 \ll 10^{-3}\,\mathrm{eV}$ the N_1 energy spectrum deviates from the thermal Fermi-Dirac distribution that we assumed. Using the slightly less accurate thermal correction to ϵ, obtained neglecting thermal motion of N_1 (dashed line in fig. 6a) typically affects the final result by a $\mathcal{O}(1)$ factor. Other minor effects might be important: the exact dispersion relation at finite temperature, thermal corrections to couplings, higher order corrections, and CP-violation in $\Delta L = 1$ scatterings.

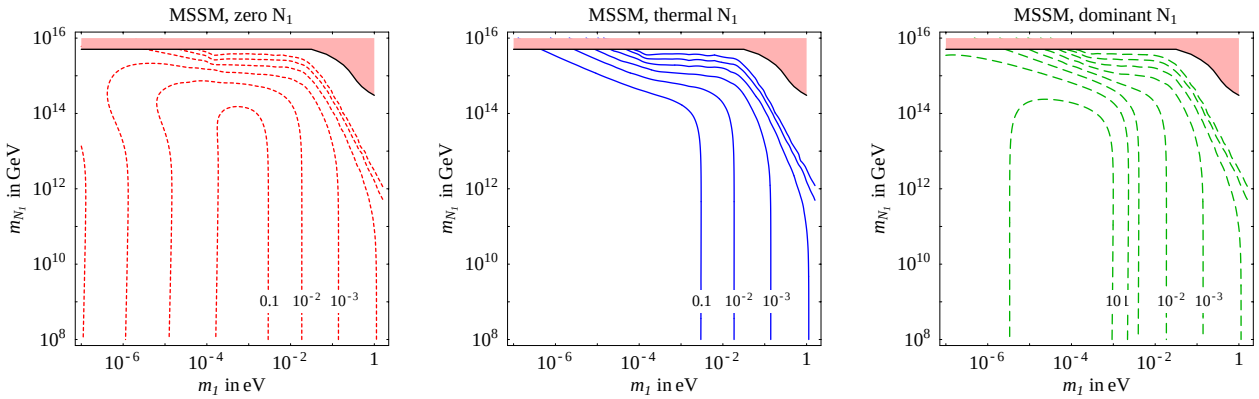

Figure 11: **Efficiency η of leptogenesis** *in the MSSM, assuming zero, thermal or dominant initial $N_1, \tilde{N}_1$ abundancy. In the shaded regions the neutrino Yukawa couplings are non-perturbative.*

On the other side, a full computation might be not necessary. Including only the thermal effects which in the SM turn out to be dominant as discussed in section 4.1, could be a good approximation also for the MSSM. Therefore we do not compute all relevant cross sections including finite temperature effects, but we adopt the MSSM cross sections of ref. [30], inserting the temperature-dependent top Yukawa coupling and Higgs boson mass in IR-enhanced processes, and performing a correct subtraction of on-shell resonances (which again reduces N_1-mediated washout scatterings by a 3/2 factor). Thermal corrections to N_1 and $\tilde{N}_1$ decays and their CP-asymmetries are computed in appendix D neglecting the thermal motion of N_1, $\tilde{N}_1$ (in the SM case this would not be a very good approximation at small $\tilde{m}_1$). Finally, we do not include $\Delta L = 1$ scatterings involving gauge bosons and gauginos.

Our MSSM results have been obtained under these approximations, assuming moderately large values of $\tan\beta \sim 10$. Low-energy thresholds make the top Yukawa coupling at high energy uncertain by about a factor of 2, as discussed in ref. [21].

Proceeding as in the case of the SM, we find that the asymmetry generated in the MSSM is

$$Y_{\mathcal{B}-\mathcal{L}} = -\eta\,\epsilon_{N_1}(Y^{\rm eq}_{N_1} + Y^{\rm eq}_{\tilde{N}_1})(T \gg m_{N_1}), \tag{42}$$

where ϵ_{N_1} is the neutrino (or sneutrino) CP-asymmetry at low temperature (equal for lepton and slepton final states) [25],

$$\epsilon_{N_1} = \frac{1}{8\pi}\sum_{j\neq 1}\frac{{\rm Im}\left[(Y^\dagger Y)^2_{j1}\right]}{[Y^\dagger Y]_{11}} g\left(\frac{m^2_{N_j}}{m^2_{N_1}}\right), \tag{43}$$

$$g(x) = -\sqrt{x}\left[\frac{2}{x-1} + \ln\left(\frac{1+x}{x}\right)\right] \stackrel{x\gg 1}{\longrightarrow} -\frac{3}{\sqrt{x}}. \tag{44}$$

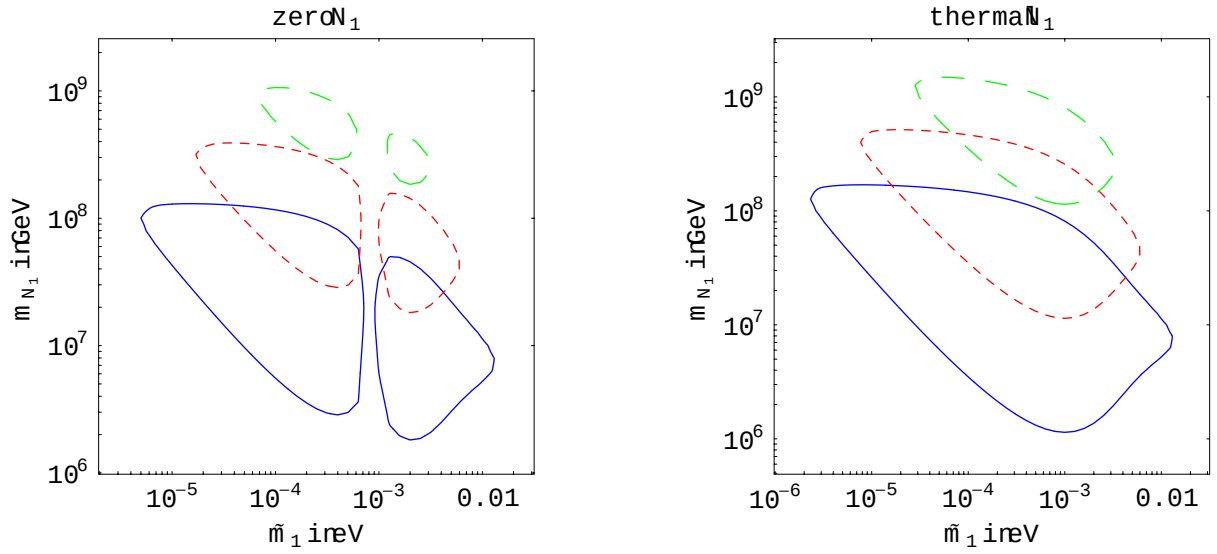

Figure 12: *Regions of* $(\tilde{m}_1, m_{N_1})$ *plane where* **soft leptogenesis** *can produce the observed baryon asymmetry for* $\mathrm{Im}A <$ TeV *and* $\sqrt{Bm_{N_1}} = 100\,\mathrm{GeV}$ *(solid line),* 1 TeV *(dashed),* 10 TeV *(long-dashed) We have assumed a vanishing (left) or thermal (right) initial sneutrino density.*

The number of effective degrees of freedom in the MSSM without right-handed neutrinos is $g_* = 228.75$. Using eq. (36) with $n_H = 2$, we obtain

$$\frac{n_{\mathcal{B}}}{s} = -1.48 \times 10^{-3} \epsilon_{N_1} \eta. \tag{45}$$

The MSSM results, analogous to those obtained from the SM and previously discussed, shown in figs. 9–11, are similar to their corresponding SM results. It is difficult to compare with previous results, which have not been presented in a systematic way.

Extra signals may come from lepton flavour violating decays like $\mu \to e\gamma$, induced in supersymmetric see-saw models by the (unknown) neutrino Yukawa couplings [31]. Some predictive minimal models allow to predict these rates in terms of the measured neutrino masses and baryon asymmetry. For example, using our revised leptogenesis computation, the prediction of ref. [32] for $\mathrm{BR}(\mu \to e\gamma)$ gets lowered by one order of magnitude.

Soft leptogenesis

"Soft leptogenesis" [10, 11] is a supersymmetric scenario of leptogenesis which requires only one heavy right-handed neutrino. The interference between the CP-odd and CP-even states of the heavy scalar neutrino resembles very much the neutral kaon system. The mass splitting as well as the required CP violation in the heavy sneutrino system comes from the soft supersymmetry breaking A and B terms, respectively associated with the Yukawa coupling and mass term of N_1. The non-vanishing value of the generated lepton asymmetry is a pure thermal effect, since at $T = 0$ the generated lepton asymmetry in leptons exactly cancels the one in sleptons.

Here we improve the results of ref. [11], taking into account thermal, Pauli blocking and stimulated emission corrections to $N_1, \tilde{N}_1$ branching ratios (which significantly enhance decays into bosons) to their CP asymmetries (computed in appendix D including thermal corrections, but neglecting the thermal motion of $N_1, \tilde{N}_1$). We recall that in this scenario $\epsilon_{\tilde{N}\to L\tilde{H}}$ has an opposite sign to $\epsilon_{\tilde{N}\to\tilde{L}H}$, and [11]

6 Leptogenesis with reheating of the universe

By now there is a wide consensus that the early universe underwent a primordial stage of inflation [33] responsible for the observed homogeneity and isotropy of the present universe, as well as for the generation of the cosmological perturbations.

The radiation–dominated era of the universe is usually assumed to be originated by the decay of the coherent oscillations of a scalar field, the inflaton field, whose vacuum energy has driven inflation For such a reason the reheating process is often associated with the final stage of inflation. However, we point out that reheating could have been episodic, with several reheat events after inflation. We will be interested in the final reheating which may just as well have been the result of the decay of a weakly coupled scalar field unrelated to inflation, for instance a modulus. For this reason the scalar field ϕ, whose decay leads to reheating, will not be referred to as the inflaton.

The decay of the scalar field ϕ into light degrees of freedom and their subsequent thermalization, called reheating, leaves the universe at a temperature $T_{\rm RH}$, which represents the largest temperature of the plasma during the subsequent radiation–dominated epoch, when temperature is a decreasing function of time. The onset of the radiation dominated era is in fact placed at the temperature $T_{\rm RH}$, *i.e.* at the end of the reheating phase.

Usually $T_{\rm RH}$ is assumed to be very large and this is the assumption we have made in the previous sections. However the only information we have on the smallest value of $T_{\rm RH}$ is from requiring a successful period of primordial nucleosynthesis, $T_{\rm RH} \gtrsim 1$ MeV. Therefore, from a phenomenological point of view, $T_{\rm RH}$ is actually a free parameter[8]. Any scenario of baryogenesis based on the out-of-equilibrium decay of some heavy particle depends crucially on the assumption that these particles were generated during the reheating process with abundances sufficiently large to generate the observed baryon asymmetry. During reheating, particles are generated through thermal scatterings and quickly thermalize. Among them, right-handed neutrinos may be also produced but their number depends strongly on the reheating temperature. If the latter is too small, the thermal bath does not give rise to a number of right-handed neutrinos large enough to produce the observed baryon asymmetry. This leads to a lower limit on $T_{\rm RH}$. Computing this lower bound is the goal of this section.

During the reheating epoch, the energy density of the universe is dominated by the

[8]Low reheating scenarios lead as well to a new perspective on baryogenesis [34], to the possibility that massive neutrinos may play the role of warm dark matter [35] or to a change in the predictions of the relic abundance and resulting model constraints of supersymmetric dark matter, axions, massive neutrinos, and other dark matter candidates [36, 37].

coherent oscillations of a scalar field ϕ. Considering for the moment the case of small abundance of right-handed neutrinos[9], as a first step we assume that the dynamics of reheating is described by the Boltzmann equations for the energy densities $\rho_{\phi,R}$ of the two coupled components: the unstable massive field ϕ and the radiation R [38, 39, 36]

$$\frac{d\rho_\phi}{dt} = -3H\rho_\phi - \Gamma_\phi \rho_\phi \,, \tag{46}$$

$$\frac{d\rho_R}{dt} = -4H\rho_R + \Gamma_\phi \rho_\phi \,, \tag{47}$$

where $H = \dot{a}/a = \sqrt{8\pi(\rho_\phi + \rho_R)/3M_{\rm Pl}^2}$, and $M_{\rm Pl}$ is the Planck mass. Here we have assumed that the relativistic decay products of the scalar field rapidly thermalize and form a relativistic bath of temperature T (for a discussion about this point see Ref. [39]). The key point of our considerations is that reheating is not an instantaneous process. On the contrary, the radiation-dominated phase follows a prolonged stage of matter domination during which the energy density of the universe is dominated by the coherent oscillations of the field ϕ. The oscillations start at time H_I^{-1} and end when the age of the universe becomes of order of the lifetime Γ_ϕ^{-1} of the scalar field. At times $H_I^{-1} \lesssim t \lesssim \Gamma_\phi^{-1}$ the dynamics of the system is quite involved. During this stage the energy density per comoving volume of the ϕ field decreases as $\exp(-\Gamma_\phi t)$ and the light decay products of the scalar field thermalize. The temperature T of this hot plasma, however, does not scale as $T \propto a^{-1}$ as in the ordinary radiation-dominated phase (where a is the Friedmann–Robertson–Walker scale factor) [38, 39], but reaches a maximum $T_{\rm MAX} \sim (H_I M_{\rm Pl})^{1/4} T_{\rm RH}^{1/2}$ and then decreases as $T \propto a^{-3/8}$, signalling the continuous release of entropy from the decays of the scalar field.

In fact, until $t \ll \Gamma_\phi^{-1}$ assuming $\rho_\phi \gg \rho_R$ the system approximately evolves as

$$\rho_\phi(t) = \rho_\phi(0)(a_0/a(t))^3 e^{-\Gamma_\phi t} \tag{48}$$

$$\rho_R(t) \equiv \frac{\pi^2 g_*}{30} T^4 \approx \frac{\sqrt{6/\pi}}{10} \Gamma_\phi M_{\rm Pl} \sqrt{\rho_\phi} \left[1 - (a_0/a)^{5/2}\right] . \tag{49}$$

This scaling continues until the time $t \sim \Gamma_\phi^{-1}$, when the radiation-dominated phase starts with temperature $T \sim T_{\rm RH}$, defined as

$$T_{\rm RH} = \left[\frac{45}{4\pi^3 g_*\left(T_{\rm RH}\right)}\, \Gamma_\phi^2 M_{\rm Pl}^2\right]^{1/4} . \tag{50}$$

The process is described by two extra parameters, $\rho_\phi(0)$ and Γ_ϕ. It is convenient to replace them with the maximal and reheating temperatures, $T_{\rm MAX}$ and $T_{\rm RH}$. Before reheating is completed, at a given temperature, the universe expands faster than in the radiation-dominated phase. Notice that $T_{\rm RH}$ is not the maximum temperature during the reheat process. On the contrary, $T_{\rm MAX}$ can be much larger than $T_{\rm RH}$.

During reheating right-handed neutrinos may be produced in several ways. They can be generated directly through the scalar field perturbative decay process [40] (this requires that the mass of the ϕ-field is larger than m_{N_1}) or through nonperturbative processes taking

[9]The case of non-negligible N_1 density is discussed in appendix A.

place at the preheating stage [41, 42]. These mechanisms, however, introduce new unknown parameters such as the coupling of right-handed neutrinos to ϕ. In this section we take a more conservative point of view and we limit ourselves to the case in which right-handed neutrinos are produced by thermal scatterings during the reheat stage, so that in the limit $T_{\rm RH} \gg m_{N_1}$ we obtain the case (0) studied in section 4 (in the opposite case of dominant inflaton decay into N_1, the $T_{\rm RH} \gg m_{N_1}$ limit is given by case (∞) of section 4). For the sake of concreteness we will focus on the leptogenesis scenario, but our findings can be easily generalized to any out-of-equilibrium scenario. Furthermore, we assume that the mass of the inflaton field is larger than the reheating temperature $T_{\rm RH}$; for a discussion of the opposite case, see ref. [43].

We now generalize the Boltzmann equations for thermal leptogenesis including reheating. In the standard case it is convenient to write the Boltzmann equations that dictate the time evolution of the number densities $n_X(t)$ of any species X in terms of $Y_X(z) \equiv n_X/s$ where $z \equiv m_N/T$. In fact, while particle densities n_X strongly depend on t because of the expansion of the universe, their ratios with respect to the entropy density s remain constant in the absence of interactions. Since the temperature T is a monotonic decreasing function, one usually replaces the time t with T.

These two statements no longer hold during reheating. Nevertheless, we still find convenient to write the Boltzmann equations for leptogenesis in terms of $Y_X(z)$. The first pre-heating phase (when T grows from zero to $T_{\rm MAX}$) is so fast that it gives no contribution to leptogenesis: the interesting dynamics happen during the second reheating phase, when the temperature decreases in a non standard characteristic way, $T \propto a^{-3/8}$. Therefore *corrections to leptogenesis are fully described by a single parameter, the reheating temperature* $T_{\rm RH}$, as long as $T_{\rm MAX}$ is sufficiently larger than m_{N_1}.

Since the temperature is defined in terms of the radiation density by eq. (47), we can write

$$\frac{d}{dt} = -4HZ\rho_R \frac{d}{d\rho_R} = HZz\frac{d}{dz} \qquad Z \equiv 1 - \frac{\Gamma_\phi \rho_\phi}{4H\rho_R} = -\frac{a}{T}\frac{dT}{da}. \tag{51}$$

Z vanishes when the maximal temperature $T_{\rm MAX}$ is reached, then $Z \simeq 3/8$ during reheating, and finally $Z \simeq 1$ in the standard radiation-dominated phase. Apart from this $\mathcal{O}(1)$ correction, reheating affects leptogenesis in two main ways 1) H has a non-standard expression: ρ_ϕ induces a faster expansion 2) ϕ decays create additional matter. The Boltzmann equations for leptogenesis are explicitly written in appendix A, eq. (69).

Results

Figure 13 shows η as function of $\tilde{m}_1$ and of $m_{N_1}/T_{\rm RH}$. Although it has been obtained for $m_{N_1} = 10^{10}\,\text{GeV}$, other values of $m_{N_1} < 10^{14}\,\text{GeV}$ would essentially give the same result.

We see that the final baryon asymmetry is strongly suppressed if $T_{\rm RH} \ll m_{N_1}$. This is due to entropy release from inflaton decays, which gives a $\sim (m_{N_1}/T_{\rm RH})^5$ suppression of η. Furthermore during reheating the universe expands faster than during the standard thermal phase: $H/H_{\rm standard} \approx (T/T_{\rm RH})^2$. This makes both N_1 production and washout less efficient, increasing the value of $\tilde{m}_1$ at which leptogenesis is maximally efficient, as can be seen in fig. 13.

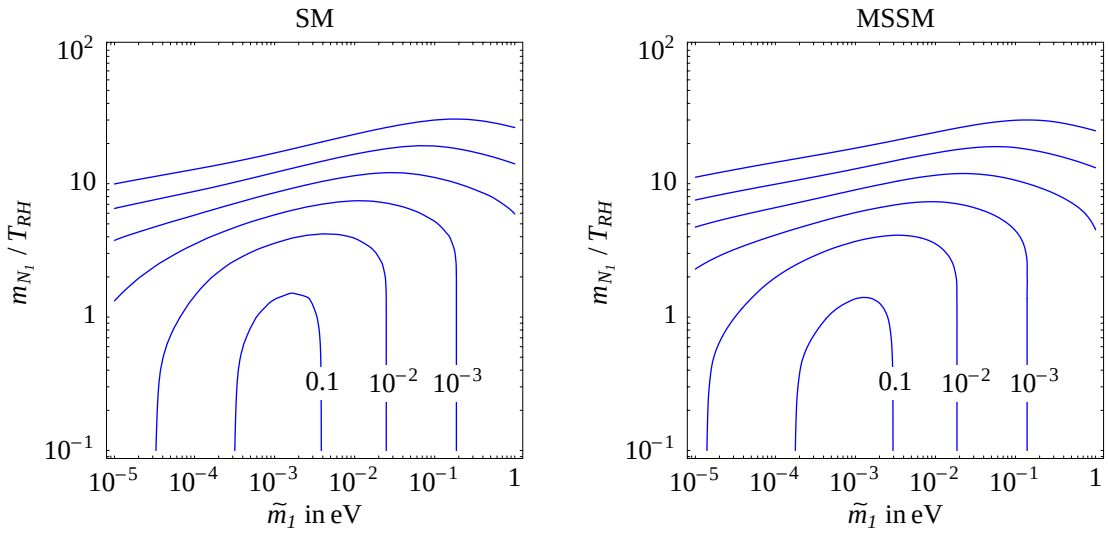

Figure 13: *Isocurves of the efficiency parameter* $\eta = 10^{-6,-5,\ldots,-1}$ *for leptogenesis with reheating as function of* $(\tilde{m}_1, m_{N_1}/T_{\rm RH})$ *in the SM (left) and MSSM (right) for* $m_{N_1} = 10^{10}\,{\rm GeV}$ *(the plot would be only slightly different for any* $m_{N_1} \ll 10^{14}\,{\rm GeV}$*).*

Making use of the bound in eq. (40) [27, 9, 44] and marginalizing over $\tilde{m}_1$ we can therefore derive the bound on the reheating temperature shown in fig. 14. This bound holds assuming that thermal leptogenesis generates the observed baryon asymmetry, that the inflaton decays into SM particles rather than into right-handed neutrinos, and that right-handed neutrinos are hierarchical, $m_{N_1} \ll m_{N_{2,3}}$. In the case of the SM, the lowest reheating temperature allowed for successful leptogenesis turns out to be 2.8×10^9 GeV, while in the case of the MSSM the lowest value is 1.6×10^9 GeV. However, there are various reasons to suspect that the reheating temperature is small in locally supersymmetric theories. Indeed, gravitinos (and other dangerous relics like moduli fields) are produced during reheating. Unless reheating is delayed, gravitinos will be overproduced, leading to a large undesired entropy production when they decay after big-bang nucleosynthesis [45]. The limit from gravitino overproduction is $T_{\rm RH} \lesssim 10^9$ to 10^{10}GeV, or even stronger [46]. This upper bound is at odds with the lower bound we have computed to achieve successful leptogenesis. Fig. 9b shows that this conflict can be avoided if N_1 and/or $\tilde{N}_1$ decayed while giving a substantial contribution to the total energy density of the universe and $\tilde{m}_1 \sim \tilde{m}_1^*$. In such a situation leptogenesis depends on the precise value of the initial $N_1, \tilde{N}_1$ abundancy, unless it is dominant. It can be realized if the inflaton decays dominantly into right-handed (s)neutrinos, or if $\tilde{N}_1$ acquires a large vacuum expectation value, as discussed in the next subsection. An alternative solution to solve the gravitino problem, maintaining a thermal abundance of $\tilde{N}_1$, is to rely on "soft leptogenesis" [11].

We can further elaborate on the results presented in figures 13, 14 by making simple analytical approximations. Since we are interested in the effects of reheating, we consider

the case $m_{N_1} > T_{\rm RH}$, and since we are studying lower bounds on $T_{\rm RH}$, we restrict ourselves to the most favorable case in which $T_{\rm MAX} > m_{N_1}$.

The efficiency factor η receives three kinds of contributions,

$$\eta = \eta_{\rm ab}\eta_{\rm eq}\eta_{\rm RH}. \tag{52}$$

Here $\eta_{\rm ab}$ measures the N_1 abundance before decay, relative to the equilibrium density. In order to estimate it, we first define

$$K(T) = \frac{\Gamma}{H}, \tag{53}$$

where Γ is the N_1 decay rate ($\Gamma = (G_F \tilde{m}_1 m_{N_1}^2)/(2\sqrt{2}\pi)$ at $T \ll m_{N_1}$ and $\Gamma = (G_F \tilde{m}_1 m_{N_1}^3)/(2\sqrt{2}\pi T)$ at $T \gtrsim m_{N_1}$) and H is the Hubble constant, with $H = [5\pi^3 g_*^2(T)]/[9 g_*(T_{\rm RH})]^{1/2} T^4/(T_{\rm RH}^2 M_{\rm Pl})$. Under the assumption[10] that the right-handed neutrino density n_{N_1} is much smaller than the equilibrium density $n_{N_1}^{\rm eq}$, and taking the inverse decay as the dominant production process, in the relativistic limit we obtain [36]

$$\frac{d(n_{N_1}/T^8)}{dT} = -\frac{8}{3} K \frac{n_{N_1}^{\rm eq}}{T^9}. \tag{54}$$

Using $K \propto T^{-5}$ and $n_{N_1}^{\rm eq} \propto T^3$, we find

$$\frac{n_{N_1}}{n_{N_1}^{\rm eq}} = \frac{4}{15} K. \tag{55}$$

Next, we define

$$K_* \equiv K(m_{N_1}) = \frac{\tilde{m}_1}{3 \times 10^{-3}\ {\rm eV}} \left(\frac{T_{\rm RH}}{m_{N_1}}\right)^2. \tag{56}$$

If $K_* \gg 1$, the right-handed neutrinos reach the equilibrium density before they become non-relativistic and $\eta_{\rm ab} = 1$. If $K_* \ll 1$, from eq. (55) we obtain $\eta_{\rm ab} = (4/15) K_*$.

The next coefficient in eq. (52) is $\eta_{\rm eq}$, which measures the out-of-equilibrium condition at decay. If $K_* \ll 1$, the right-handed neutrino is decoupled when it becomes non-relativistic, and $\eta_{\rm eq} = 1$. If $K_* \gg 1$, $\eta_{\rm eq}$ can be estimated by computing the N_1 density at the temperature T_f at which the processes that damp the baryon asymmetry go out of equilibrium,

$$\eta_{\rm eq} = \frac{\sqrt{2\pi}}{3\zeta(3)} \left(\frac{m_{N_1}}{T_f}\right)^{3/2} e^{-m_{N_1}/T_f}. \tag{57}$$

We assume that the dominant process erasing the asymmetry is the inverse decay, with $\Gamma_{\rm ID} = (m_{N_1}/T)^{3/2} \exp(-m_{N_1}/T) G_F \tilde{m}_1 m_{N_1}^2/(8\sqrt{\pi})$. Then T_f is given by the condition

$$\Gamma_{\rm ID} = H|_{T=T_f}\,. \tag{58}$$

[10]The expression we are using for Γ is not correct at high temperatures, where the Higgs decay is the relevant process. However, for this qualitative discussion, the approximation is adequate, since the right-handed production is dominated at temperatures $T \sim m_{N_1}$, where we can take $\Gamma = (G_F \tilde{m}_1 m_{N_1}^3)/(2\sqrt{2}\pi T)$.

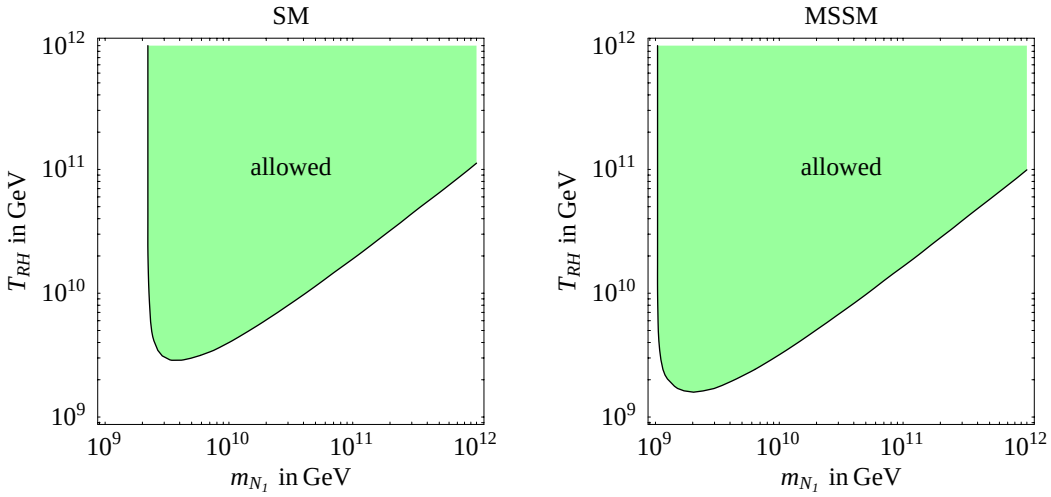

Figure 14: *Lower bounds on m_{N_1} and $T_{\rm RH}$ from leptogenesis in the SM and MSSM.*

If $T_f > T_{\rm RH}$, eq. (58) corresponds to $K_*(m_{N_1}/T_f)^\beta \exp(-m_{N_1}/T_f) \simeq 1$, with $\beta = 11/2$ which, in the range $1 \ll K_* < 10^4$ is approximately solved by $m_{N_1}/T_f \simeq a(\ln K_*)^b$, with $a = 10$ and $b = 0.5$. If $T_f < T_{\rm RH}$, the usual radiation-dominated epoch determines the dynamics and we find an analogous solution with $\beta = 7/2$, $a \approx 5$, $b \approx 0.5$, and K_* must be computed using the usual Hubble parameter $H \propto T^2$.

Finally, $\eta_{\rm RH}$ measures the dilution caused by the expansion during the reheating phase. Therefore $\eta_{\rm RH} = (T_{\rm RH}/m_{N_1})^5$ for $K_* \ll 1$, $\eta_{\rm RH} = (T_{\rm RH}/T_f)^5$ for $K_* \gg 1$ and $T_f > T_{\rm RH}$, and $\eta_{\rm RH} = 1$ for $K_* \gg 1$ and $T_f < T_{\rm RH}$.

Putting together the different contributions to η, we obtain, for $T_f > T_{\rm RH}$

$$\eta \approx 0.1 \left(\frac{\tilde{m}_1}{10^{-3}\ \text{eV}}\right)\left(\frac{T_{\rm RH}}{m_{N_1}}\right)^7 \qquad \text{for } \ \tilde{m}_1 \ll 3\times 10^{-3}\ \text{eV}\left(\frac{m_{N_1}}{T_{\rm RH}}\right)^2 \quad (59a)$$

$$\eta \approx 20 \left(\frac{10^{-3}\ \text{eV}}{\tilde{m}_1}\right)\left(\frac{T_{\rm RH}}{m_{N_1}}\right)^3 (\ln K_*)^{0.5} \qquad \text{for } \ \tilde{m}_1 \gg 3\times 10^{-3}\ \text{eV}\left(\frac{m_{N_1}}{T_{\rm RH}}\right)^2 . \quad (59b)$$

Leptogenesis from inflaton sneutrino decays

In supersymmetric seesaw models there is a distinctive possibility that inflaton itself is a scalar superpartner of the lightest heavy neutrino [47, 48]. This is an interesting scenario because both the reheating of the Universe and the thermal leptogenesis efficiency depend on a single neutrino parameter $\tilde{m}_1$. Therefore this is a predictive example of a realistic scenario of the early universe. In this case there is an additional source of the lepton asymmetry from the direct decays of the inflaton sneutrino.

We do not study in detail how the sneutrino condensate decays, and assume a decay width $\Gamma_\phi = \Gamma_{\tilde{N}_1}(T = 0)$ with CP asymmetry $\epsilon_1 = \epsilon_{\tilde{N}_1}(T = 0)$. This is not correct if $T_{\rm RH} \gtrsim m_{N_1}$ [43], that, in our case, happens for $\tilde{m}_1 \gtrsim 10^{-3}\,$eV. However if $\tilde{m}_1 \gtrsim 10^{-2}\,$eV thermalization is so efficient that details of the past thermal history negligibly affect our

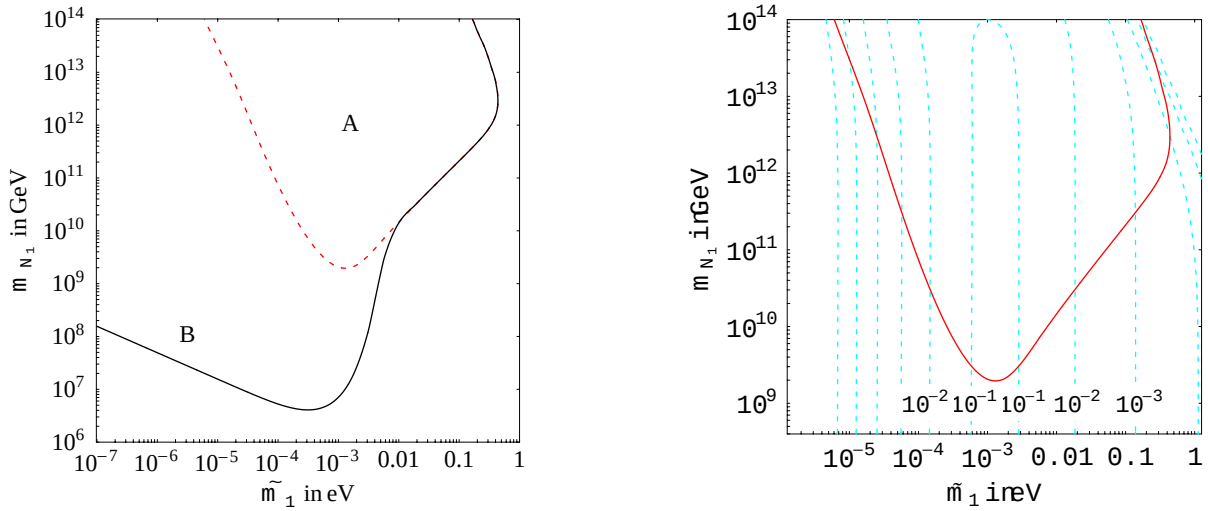

Figure 15: *Lower bounds on m_{N_1} from sneutrino inflaton leptogenesis (left) and the efficiency of thermal leptogenesis in this scenario (right).*

final result.

In order to study this scenario we solved the Boltzmann equations for the $\tilde{N}_\pm \equiv \tilde{N}_1 \pm \tilde{N}_1^\dagger$ and N_1 abundancies, and for the $\tilde{N}_1$ condensate. In our calculation we take into account the temperature dependent interaction rates and CP asymmetries, and the on-shell resonances are correctly subtracted. The Hubble constant H and the parameter Z are the obvious supersymmetric extensions of eq.s (69–**??**) including the reheating effects of thermal (s)neutrinos.

Assuming as before hierarchical light neutrinos and using the maximal CP asymmetry of eq. (40) for supersymmetric case, the solutions to the Boltzmann equations are presented in fig. 15 where we plot the lower bound on m_{N_1} as a function of $\tilde{m}_1$ from the observed baryon asymmetry of the Universe. This parameter space has two distinct regions. The one denoted by **A** is the region of purely thermal leptogenesis. The corresponding curve in [49] was obtained with wrong subtraction of on-shell resonances and with a constant CP asymmetry. For the region **A** we plot also the isocurves of the leptogenesis efficiency η (right plot) which decreases very fast for small $\tilde{m}_1$. This is because of the suppression of T_{RH} in that region of the parameter space.

The region denoted by **B** is the one of direct leptogenesis from the inflaton decay [48].

Between those two regions leptogenesis is a mixture of the two scenarios. Thus the inflaton sneutrino scenario allows to lower the lower bound on m_{N_1} and on T_{RH} from successful leptogenesis over a large region of $\tilde{m}_1$. This is very desirable from the point of view of the gravitino problem, as discussed in the previous subsection.

7 Conclusions

We have performed a thorough study of thermal leptogenesis which, at present, is one of the most attractive mechanism to account for the baryon asymmetry of the universe. The final prediction of leptogenesis for the baryon asymmetry can be written in terms of the CP-asymmetry at zero temperature, ϵ_{N_1}, and of the efficiency η of leptogenesis as $n_{\mathcal{B}}/s = -1.37\ 10^{-3}\epsilon_{N_1}\eta$ in the SM, and as in eq. (45) for the MSSM. Figures 8 (SM) and 11 (MSSM) show η as function of the relevant unknown high energy parameters, *i.e.* the mass m_{N_1} of the lightest right-handed neutrino N_1 and $\tilde{m}_1$, its contribution to light neutrino masses. All the new effects discussed in this paper have been added: cumulatively the final baryon asymmetry gets typically corrected by a order unity factor with respect to previous studies. For example, $n_{\mathcal{B}}$ gets roughly doubled if $\tilde{m}_1 \sim (\Delta m^2_{\rm atm,sun})^{1/2}$. Since individual terms give larger corrections to the final result, in general, it is necessary to include these corrections to obtain a trustworthy result. The most important sources of corrections are summarized in section 4.1.

Although thermal leptogenesis allows to compute the baryon asymmetry in terms of particle physics, a few relevant parameters are presently unknown. Improving on this issue is as crucial as hard. In the meantime, by making some assumptions on the high-energy parameters (the most relevant one being that right-handed neutrinos are hierarchical) one can get interesting constraints [27, 9]. Including all the new effects discussed in this paper and combining uncertainties at 3σ, we have found that successful leptogenesis needs

$$m_{N_1} > \begin{cases} 2.4 \times 10^9\,\text{GeV} & \text{if } N_1 \text{ has zero} \\ 4.9 \times 10^8\,\text{GeV} & \text{if } N_1 \text{ has thermal} \\ 1.7 \times 10^7\,\text{GeV} & \text{if } N_1 \text{ has dominant} \end{cases} \quad \text{initial abundancy at } T \gg m_{N_1}$$

and $m_3 < 0.13\,\text{eV}$, where m_3 is the heaviest left-handed neutrino mass. In the MSSM we get similar values.

Furthermore, in inflationary cosmologies, we obtained a lower bound on the reheating temperature, $T_{\rm RH} > 2.8 \times 10^9\,\text{GeV}$ assuming that inflaton reheats SM particles but not directly right-handed neutrinos. Within the MSSM the bound is $T_{\rm RH} > 1.6 \times 10^9\,\text{GeV}$, which is at odds with the lower bound from gravitino overproduction. This seems to suggest that one has to rely on alternative (non-thermal) mechanisms to generate right-handed (s)neutrinos after inflation (like the sneutrino condensate studied at page 31), or to invoke leptogenesis with degenerate right-handed neutrinos [50, 29] or "soft leptogenesis" [11] (that we study at page 25).

We stress that all these constraints are based on untested assumptions and therefore cannot be considered as absolute bounds.

* * *

Finally, we would like to emphasize some weak points and possible refinements of our analysis. At $\tilde{m}_1 \gg 10^{-3}\,\text{eV}$ the relevant abundances are close to thermal equilibrium, suppressing the dependence on initial conditions. In this region we are not aware of any missing effect larger than $\sim 10\%$. Our inclusion of thermal effects focussed on thermal

corrections to kinematics: by resumming corrections to propagators we could study effects which become large at $T \gtrsim m_{N_1}$. We approximately included corrections to couplings by renormalizing them at $\sim 2\pi T$. Although this is a significant improvement with respect to previous computations which used couplings renormalized at the weak scale, a somewhat different approach could give a more precise result valid for $\tilde{m}_1 \gg 10^{-3}\,\text{eV}$. As explained in the text, one should concentrate on computing corrections to the $N_1 \to HL$ decay rate at relatively small temperature, $T \lesssim m_{N_1}$, without making our simplifying approximations, with the goal of including all few % corrections of relative order $\sim g^2/\pi^2$ and λ_t^2/π^2: $\Delta L = 1$ scatterings and their CP-asymmetry, three-body decays $N_1 \to LQ_3U_3, LHA$ and radiative corrections to $N_1 \to LH$ decay and its CP-asymmetry.

At $\tilde{m}_1 \lesssim 10^{-3}\,\text{eV}$ the final result depends on initial conditions. Starting with zero initial abundancy, the final baryon asymemtry also depends strongly on thermal corrections to the CP-asymmetry ϵ_{N_1}. Unfortunately we found that, as the temperature rises, thermal corrections first reduce, then enhance, reduce and finally enhance ϵ_{N_1}. Since the correction does not go in a clear direction, a more accurate computation might be welcome.

Acknowdlegements We thank R. Barbieri, S. Catani, M. Ciafaloni, S. Davidson, M. Mangano, S. Moretti, M. Papucci, M. Passera, M. Plümacher, R. Rattazzi, T. Hambye, F. Vissani.

A Boltzmann equations

Elastic scatterings keep the SM particles in *kinetic* equilibrium, so that their energy distribution approximatively follows the Maxwell-Boltzmann distribution $f = e^{-E/T}$ (unless otherwise specified we neglect the slightly different energy distributions of bosons and fermions. This is a good approximation because $f \lesssim 0.05$ at the average energy $\langle E \rangle \sim 3T$). Each particle species is simply characterized by its total abundancy, that can be varied only by inelastic processes. When they are sufficiently fast to maintain also *chemical* equilibrium, the total number n^{eq} and energy density ρ^{eq} of ultra-relativistic particles at temperature T are

$$n^{\text{eq}} = g \int d^3p (2\pi)^3 \; f = \frac{gT^3}{\pi^2}, \qquad \rho^{\text{eq}} = g \int d^3p (2\pi)^3 \; E f^{\text{eq}} = \frac{3gT^4}{\pi^2}$$

where g is the number of spin degrees of freedom. All SM particles have $g_{\text{SM}} = 118$, and a right handed neutrino has $g_N = 2$.

In kinetic equilibrium, the phase space density is fn/n^{eq}. The Boltzmann equation describing the evolution of the total abundancy n_N of a particle N is

$$\dot{n}_N + 3Hn_N = -\sum_{a,i,j,\ldots} [Na\cdots \leftrightarrow ij\cdots], \tag{60}$$

where $H = \dot{a}/a = \sqrt{8\pi\rho/3M_{\text{Pl}}^2}$,

$$[Na\cdots \leftrightarrow ij\cdots] = n_N n_a \ldots n_N^{\text{eq}} n_a^{\text{eq}} \ldots \gamma^{\text{eq}}(Na\cdots \to ij\cdots) - n_i n_j \cdots n_i^{\text{eq}} n_j^{\text{eq}} \cdots \gamma^{\text{eq}}\,(ij\cdots \to Na\cdots)\,.$$

A symmetry factor should be added when there are identical particles. $\gamma^{\rm eq}$ is the space-time density of scatterings in thermal equilibrium of the various interactions in which a N particle takes part:

Having neglected Pauli-blocking and stimulated emission factors, and assuming that $|A|^2$ does not depend on the relative motion of particles with respect to the plasma, the expression for the scattering rates $\gamma^{\rm eq}$ can be conveniently simplified.

For a decay, eq. (**??**) reduces to

The thermal rate $\gamma^{\rm eq}$ of a two-body scattering can be conveniently rewritten by multiplying eq. (**??**) times $1 = \int d^4P \int \delta^4(P - P_N - P_a)$

The $3H$ term in the Boltzmann equations, eq. (60), accounts for the dilution due to the overall expansion of the universe. It is convenient to reabsorb it by normalizing the number density n to the entropy density s. Therefore we study the evolution of $Y = n/s$ as function of $z = m_N/T$ in place of time t ($H\,dt = d\ln R = d\ln z$ since during adiabatic expansion sR^3 is constant, i.e. $R \propto 1/T$). The Boltzmann equations become

$$zHs\frac{dY_N}{dz} = -\sum_{a,i,j,\ldots}[Na \leftrightarrow ij]. \tag{61}$$

Leptogenesis

We now specialize to leptogenesis. Neglecting sphalerons, the scattering processes relevant for leptogenesis are:[11]

We assume that N_1, L and $\bar{L}$ can be out of thermal equilibrium, while $Y_X = Y_X^{\rm eq}$ for $X = \{H, Q_3, U_3\}$. The Boltzmann equations are

$$\begin{aligned} zHsY'_{N_1} &= -D - \bar{D} - S_s - \overline{S_s} - S_t - \overline{S_t} \\ zHsY'_{L} &= D - N_s - N_t - S_s + \overline{S_t} \\ zHsY'_{\bar{L}} &= \bar{D} + N_s - \overline{N_t} - \overline{S_s} + S_t. \end{aligned}$$

We write the decay rates in terms of the CP-conserving total decay rate γ_D and of the CP-asymmetry $\epsilon_{N_1} \ll 1$:

$$\begin{aligned} \gamma^{\rm eq}(N_1 \to LH) = \gamma^{\rm eq}(\bar{L}\bar{H} \to N_1) = (1 + \epsilon_{N_1})\gamma_D/2, \\ \gamma^{\rm eq}(N_1 \to \bar{L}\bar{H}) = \gamma^{\rm eq}(LH \to N_1) = (1 - \epsilon_{N_1})\gamma_D/2 \end{aligned} \tag{62}$$

[11] We add $\Delta L = 1$ scatterings involving gauge bosons. We neglect three-body decays $N_1 \to LQ_3U_3, LHA$ and radiative corrections to $N_1 \to LH$ decay and its CP-asymmetry, although in most of the parameter space they enter at the same order as $\Delta L = 1$ scatterings, giving $\sim g^2/\pi^2 \sim$ few % corrections. Ref. [29] suggests that $\Delta L = 1$ scatterings have, at $T = 0$, the same CP-asymmetry as decays. If true this gives % corrections, that we prefer not to include.

so that

$$D = \frac{\gamma_D}{2}\left[\frac{Y_{N_1}}{Y_{N_1}^{\rm eq}}(1+\epsilon_{N_1}) - \frac{Y_L}{Y_L^{\rm eq}}(1-\epsilon_{N_1})\right], \qquad \bar{D} = \frac{\gamma_D}{2}\left[\frac{Y_{N_1}}{Y_{N_1}^{\rm eq}}(1-\epsilon_{N_1}) - \frac{Y_{\bar{L}}}{Y_{\bar{L}}^{\rm eq}}(1+\epsilon_{N_1})\right].$$

Here $Y_{N_1}^{\rm eq}$, $Y_L^{\rm eq}$ and $Y_{\bar{L}}^{\rm eq}$ are fermionic equilibrium densities each with 2 degrees of freedom, and therefore are all equal to high temperature. Keeping only decays and inverse decays, a baryon asymmetry would be generated even in thermal equilibrium, since CPT invariance implies that if N_1 decays preferentially produce L, than inverse decays preferentially destroy $\bar{L}$ (or, in formulæ, $D-\bar{D} \neq 0$) [51]. In order to obtain Boltzmann equations with the correct behavior one needs to correctly address some subtlety, as discussed in ref. [52] in the context of baryogenesis.

Subtractions of on-shell propagators

At leading order in the couplings, $2 \leftrightarrow 2$ scatterings must be computed at tree level and are consequently CP-conserving. However N_s, the $LH \leftrightarrow \bar{L}\bar{H}$ scattering rate mediated by s-channel exchange of N_1 shown in fig. 4d, must be computed by subtracting the CP-violating contribution due to on-shell N_1 exchange, because in the Boltzmann equations this effect is already taken into account by successive decays, $LH \leftrightarrow N \leftrightarrow \bar{L}\bar{H}$. Since the on-shell contribution is $\gamma_{Ns}^{\rm on-shell}(LH \to \bar{L}\bar{H}) = \gamma^{\rm eq}(LH \to N_1){\rm BR}(N_1 \to \bar{L}\bar{H})$, where $BR(N_1 \to \bar{L}\bar{H}) = (1-\epsilon_{N_1})/2$, we obtain

$$\begin{aligned}
\gamma^{\rm eq}(LH \to \bar{L}\bar{H}) &= \gamma_{Ns} - (1-\epsilon_{N_1})^2\gamma_D/4, & (63)\\
\gamma^{\rm eq}(\bar{L}\bar{H} \to LH) &= \gamma_{Ns} - (1+\epsilon_{N_1})^2\gamma_D/4, & (64)
\end{aligned}$$

so that

$$\begin{aligned}
N_s &= \frac{Y_L}{Y_L^{\rm eq}}\gamma^{\rm eq}(LH \to \bar{L}\bar{H}) - \frac{Y_{\bar{L}}}{Y_{\bar{L}}^{\rm eq}}\gamma^{\rm eq}(\bar{L}\bar{H} \to LH) & (65)\\
&= \frac{Y_{\mathcal{L}}}{Y_L^{\rm eq}}\left(\gamma_{Ns} - \frac{\gamma_D}{4}\right) + \epsilon_{N_1}\gamma_D + \mathcal{O}(\epsilon_{N_1}^2), & (66)
\end{aligned}$$

having defined the lepton number asymmetry $Y_{\mathcal{L}} = Y_L - Y_{\bar{L}}$ and used $Y_L + Y_{\bar{L}} = 2Y_L^{\rm eq} + \mathcal{O}(\epsilon_{N_1})$. Expanding at leading order in ϵ_{N_1} gives the Boltzmann equations

$$\begin{aligned}
zHsY'_{N_1} &= -\left(\frac{Y_{N_1}}{Y_{N_1}^{\rm eq}} - 1\right)(\gamma_D + 2\gamma_{Ss} + 4\gamma_{St}) & (67)\\
zHsY'_{\mathcal{L}} &= \gamma_D\left[\epsilon_{N_1}\left(\frac{Y_{N_1}}{Y_{N_1}^{\rm eq}} - 1\right) - \frac{Y_{\mathcal{L}}}{2Y_L^{\rm eq}}\right] - \frac{Y_{\mathcal{L}}}{Y_L^{\rm eq}}\left(2\gamma_N^{\rm sub} + 2\gamma_{St} + \gamma_{Ss}\frac{Y_{N_1}}{Y_{N_1}^{\rm eq}}\right), & (68)
\end{aligned}$$

where $\gamma_N^{\rm sub} = \gamma_{Nt} + \gamma_{Ns} - \gamma_D/4$.

Alternatively, one can simply not include the decay contribution to washout of $Y_{\mathcal{L}}$ because it is already accounted by resonant decays. Then one gets

We can directly compute $\gamma_{Ns}^{\rm sub} = \gamma_{Ns} - \gamma_D/4$ by subtracting to the intermediate N_1 propagator the resonant part in the narrow-width approximation[12]

The subtraction employed in ref.s [6, 9, 29] is

$$|D_{N_1}|^2 \to |{\rm Re}D_{N_1}|^2 = |D_{N_1}|^2 - ({\rm Im}\, D_{N_1})^2 \stackrel{\Gamma_{N_1} \ll m_{N_1}}{\simeq} |D_{N_1}|^2 - \frac{1}{2}\frac{\pi}{m_{N_1}\Gamma_{N_1}}\delta(s - m_{N_1}^2)$$

which leads to $\gamma_{Ns}^{\rm sub} \simeq \gamma_{Ns} - \gamma_D/8$. This corresponds to subtracting only 1/2 of the on-shell contribution, thereby over-estimating washout by 3/2 when γ_D is the dominant process (i.e. when the neutrino Yukawa coupling is small). As shown in fig. 5, the properly subtracted rate has no spurious peaks around the resonance region, in contrast with the result of refs. [6, 9].

Sphalerons

Finally, we have to include sphaleronic scatterings, that convert the lepton asymmetry into a baryon asymmetry. This is conveniently done by converting the Boltzmann equation for $Y_{\mathcal{L}}$ into a Boltzmann equation for $Y_{\mathcal{B}-\mathcal{L}}$: since $Y_{\mathcal{B}-\mathcal{L}}$ is not affected by sphalerons we only need to find the relation between $Y_{\mathcal{B}-\mathcal{L}}$ and $Y_{\mathcal{L}}$. At temperatures larger than $10^{10}\,$GeV sphaleronic scatterings are expected to be negligibly slow with respect to the expansion rate of the universe, so that $Y_{\mathcal{L}} = -Y_{\mathcal{B}-\mathcal{L}}$. At lower temperatures sphaleronic processes keep thermal equilibrium and the relation would become $Y_{\mathcal{L}} = -(63/79)Y_{\mathcal{B}-\mathcal{L}}$ ($Y_{\mathcal{L}} = -(9/8)Y_{\mathcal{B}-\mathcal{L}}$) if all SM Yukawa couplings were large (negligible). In reality some couplings mediate equilibrium reactions ($y_t, \dots$) and some others are negligible ($y_e, \dots$) so that without making approximations one cannot ignore flavour and must proceed as in ref. [7]. In particular we stress that in order to study how the three generations share the lepton asymmetry one must consider the evolution of the full flavour 3×3 density matrix. Within 10% accuracy we may approximate $Y_{\mathcal{L}} \approx -Y_{\mathcal{B}-\mathcal{L}}$ and solve the Boltzmann equation of eq. (69c). After computing $Y_{\mathcal{B}-\mathcal{L}}$ the baryon asymmetry $Y_{\mathcal{B}}$ is obtained by means of eq. (36).

Inflaton and N_1 reheating

We now add one refinement. We described in section 6 how the Boltzmann equations are modified by the presence of a field ϕ, whose decays into SM particles reheat the universe. Proceeding along the same lines we also take into account that reheating due to N_1 decays might be non-negligible. Terms of relative order ρ_{N_1}/ρ_R are neglected in the 'standard'

[12] In numerical computations one employs any representation of $\delta(x)$ that, like $\delta(x) = (2\epsilon^3/\pi)/(x^2+\epsilon^2)^2$ and unlike $\delta(x) = (\epsilon/\pi)/(x^2+\epsilon^2)$, goes to zero faster than the propagator away from the peak. The value of ϵ can be conveniently chosen to be somewhat smaller than the width of N_1, although this is not necessary if it is narrow. In this limit, which covers almost all the parameter space where thermal leptogenesis can generate the observed baryon asymmetry, one can simply set $\Gamma_{N_1}/m_{N_1} = \epsilon$, getting the subtracted propagator of eq. (74), and assign to the width any sufficiently small value.

Boltzmann equations: in thermal equilibrium this factor is small, $\rho_{N_1}/\rho_R \lesssim g_{N_1}/g_\star \sim 0.02$ since N_1 is one out of many more SM particles. Away from thermal equilibrium it can be sizable. Including these effects, the Boltzmann equations become

$$
\begin{aligned}
HZz\frac{d\rho_\phi}{dz} &= -3H\rho_\phi - \Gamma_\phi \rho_\phi \,, && \text{(69a)}\\
sHZz\frac{dY_{N_1}}{dz} &= 3sH(Z-1)Y_{N_1} - \left(\frac{Y_{N_1}}{Y_{N_1}^{\rm eq}} - 1\right)(\gamma_D + 2\gamma_{Ss} + 4\gamma_{St}) && \text{(69b)}\\
sHZz\frac{dY_{\mathcal{B}-\mathcal{L}}}{dz} &= 3sH(Z-1)Y_{\mathcal{B}-\mathcal{L}} - \gamma_D \epsilon_{N_1}\left(\frac{Y_{N_1}}{Y_{N_1}^{\rm eq}} - 1\right) + \\
&\quad - \frac{Y_{\mathcal{B}-\mathcal{L}}}{Y_L^{\rm eq}}\left(\frac{\gamma_D}{2} + 2\gamma_N^{\rm sub} + 2\gamma_{St} + \gamma_{Ss}\frac{Y_{N_1}}{Y_{N_1}^{\rm eq}}\right) && \text{(69c)}
\end{aligned}
$$

where s and ρ_R are the entropy and energy density of SM particles,

In the next appendices we will see how thermal effects can be included by modifying the scattering rates and the CP-asymmetries, but not the form of the equation themselves.

B Thermal corrections to decays and scatterings

We present the temperature-dependent decay rates and cross sections that generate and washout the lepton asymmetry. Since we consider temperatures $T \sim m_{N_1}$ much above the electroweak scale, the thermal masses of the Higgs doublet, lepton doublet, top quarks and electroweak gauge bosons are given by [22]

$$
\begin{aligned}
\frac{m_H^2}{T^2} &= \frac{3}{16}g_2^2 + \frac{1}{16}g_Y^2 + \frac{1}{4}y_t^2 + \frac{1}{2}\lambda, && \text{(70a)}\\
\frac{m_L^2}{T^2} &= \frac{3}{32}g_2^2 + \frac{1}{32}g_Y^2, && \text{(70b)}\\
\frac{m_{Q_3}^2}{T^2} &= \frac{1}{6}g_3^2 + \frac{3}{32}g_2^2 + \frac{1}{288}g_Y^2 + \frac{1}{16}y_t^2, && \text{(70c)}\\
\frac{m_{U_3}^2}{T^2} &= \frac{1}{6}g_3^2 + \frac{1}{18}g_Y^2 + \frac{1}{8}y_t^2, && \text{(70d)}\\
\frac{m_W^2}{T^2} &= \frac{11}{12}g_2^2, \qquad \frac{m_B^2}{T^2} = \frac{11}{12}g_Y^2, && \text{(70e)}
\end{aligned}
$$

where all couplings are renormalized at the RGE scale $\mu = 2\pi T$. The Higgs boson, lepton and quark masses are functions of T, even if not explicitly denoted. We neglected their zero-temperature values. At leading order the quartic Higgs coupling λ is given in terms of the zero-temperature Higgs mass m_h as $\lambda(\mu = v) = (m_h/2v)^2$ where $v = 174\,\text{GeV}$. The top Yukawa couplings is similarly given by $y_t(\mu = v) = m_t/v$. Their RGE running is known up to next-to-leading order [54].

In the MSSM the relevant thermal masses are [22]

$$\frac{m_{\tilde{L}}^2}{T^2} = 2\frac{m_L^2}{T^2} = \frac{3}{8}g_2^2 + \frac{1}{8}g_Y^2,$$
$$\frac{m_{\tilde{Q}_3}^2}{T^2} = 2\frac{m_{Q_3}^2}{T^2} = \frac{2}{3}g_3^2 + \frac{3}{8}g_2^2 + \frac{1}{72}g_Y^2 + \frac{1}{4}\lambda_t^2,$$
$$\frac{m_{\tilde{U}_3}^2}{T^2} = 2\frac{m_{U_3}^2}{T^2} = \frac{2}{3}g_3^2 + \frac{2}{9}g_Y^2 + \frac{1}{2}\lambda_t^2.$$

Here and in the following appendix the neutrino couplings Y_ν are renormalized at the high-scale. The one-loop RGE equations for the Majorana neutrino mass matrix m_{ij} valid from the Fermi scale (below which it is not affected by quantum corrections) up to m_{N_1} are [55]

$$(4\pi)^2\frac{dm}{d\ln\mu} = m(\lambda - 3g_2^2 + 6\lambda_t^2) - \frac{3}{2}\left[m\cdot(Y_E^\dagger\cdot Y_E)^T + (Y_E^\dagger\cdot Y_E)\cdot m\right] \tag{71}$$

in the SM and

$$(4\pi)^2\frac{dm}{d\ln\mu} = m(-2g_Y^2 - 6g_2^2 + 6\lambda_t^2) + m\cdot(Y_E^\dagger\cdot Y_E)^T + (Y_E^\dagger\cdot Y_E)\cdot m \tag{72}$$

in the MSSM. Higher order effects (two-loop RGE, thresholds) are partially included in our codes. Here Y_E and λ are the charged lepton and Higgs couplings. The solution of these RGEs is described in section 3.1. The Yukawa couplings of right-handed neutrinos N_1 give extra RGE effects at scales above m_{N_1}. We neglect these effects, as large Yukawa couplings anyhow lead to an exponentially small efficiency for leptogenesis.

The N_1 mass does not receive thermal corrections, as long as we neglect the relevant neutrino Yukawa couplings, which are indeed small in most of the interesting parameter region, since $|Y_{\nu 1i}|^2 < 3\times 10^{-7}(m_{N_1}/10^{10}\text{ GeV})(\tilde{m}_1/10^{-3}\text{ eV})$. We define

$$z = \frac{m_{N_1}}{T}, \qquad x = \frac{s}{m_{N_1}^2}, \qquad a_{H,L,Q,U,W,B} = \frac{m_{H,L,Q_3,U_3,W,B}^2(z)}{m_{N_1}^2}, \qquad a_\Gamma = \frac{\Gamma_{N_1}^2}{m_{N_1}^2}, \tag{73}$$

$$D_{N_1} = \frac{1}{x - 1 + ia_\Gamma^{1/2}}, \qquad |D_{N_1}^2|^{\text{sub}} = \frac{(x-1)^2 - a_\Gamma}{[(x-1)^2 + a_\Gamma]^2} \tag{74}$$

and $\lambda[a,b,c] = (a-b-c)^2 - 4bc$.

Decays

At low temperature $m_{N_1} > m_H + m_L$ so that one has the usual N_1 decay with total width

As expected, the Boltzmann approximation is accurate at low $T \lesssim 0.1\, m_{N_1}$ and differs from the full result by a few 10% at $T \sim m_{N_1}$. Actually, for the specific SM values of the thermal masses, the Boltzmann approximation is accurate within 10%.

We stress that our inclusion of thermal effects is only approximate. In the present work we focussed on those corrections which become large at $T \gtrsim m_{N_1}$.

In particular, at sufficiently high temperature the N_1 decay becomes kinematically forbidden at higher temperature by the H thermal mass. When $m_H > m_{N_1} + m_L$, the $H \to L N_1$ decay is allowed. Its width is

$$\Gamma_H = \frac{1}{16\pi}(Y_\nu Y_\nu^\dagger)_{11} \lambda^{\frac{1}{2}}[a_H, 1, a_L] \frac{a_H - 1 - a_L}{a_H^2}\, m_H. \tag{75}$$

Despite the change in the decay process the Boltzmann equations keep the same form, with the N_1 decay rate replaced by the H decay rate.

Even including thermal effects, at intermediate temperatures all $1 \leftrightarrow 2$ and $3 \leftrightarrow 0$ processes are kinematically forbidden, so that $\gamma_D = 0$.

$\Delta L = 2$ scatterings

We now consider lepton-number violating scatterings: the $\Delta L = 2$ processes $LH^\dagger \leftrightarrow \bar{L} H$ and $LL \leftrightarrow H^\dagger H$ (middle row of fig. 4).

As explained in appendix A we compute the $LH \leftrightarrow \bar{L} H^\dagger$ subtracting the contribution from on-shell intermediate N_1, to avoid double counting with two-body decays. At low temperatures the computation is similar to the $T = 0$ case: N_1 can be on-shell in the s-channel diagram of fig. 4d so that one must replace the s-channel propagator $D_{N_1} = 1/(s - m_{N_1}^2 + i m_{N_1}\Gamma_{N_1})$ with a subtracted propagator $D^{\rm sub}$.

At high temperatures, when $H \to N_1 L$ replace $N_1 \to H L$ decays, the situation becomes more tricky. N_1 can be on-shell in the u-channel diagram of fig. 4e. As this corresponds to on-shell N_1 in the decay $H \to N_1 L$, it has to be subtracted similarly to the s-channel resonance. The imaginary part of the N_1 propagator which renders finite the $LH \leftrightarrow \bar{L} H^\dagger$ rate is no longer given by N_1 decay, but by thermal absorption of N_1, given by [56]

$$-{\rm Im}\,\Pi_{N_1}(E_N) \;=\; E_N \Gamma_{N_1}(E_N) = \frac{1}{2}\int d\vec{p}_L\, d\vec{p}_H\, (2\pi)^4 \delta^4(P_N + P_L - P_H) |A|^2 [f_L + f_H]$$

Unlike a decay at $T = 0$, for which $\Gamma_{N_1}(E_N) = \Gamma_{N_1}(m_{N_1}) m_{N_1}/E_N$, the N_1 width at finite temperature depends on thermal motion of N_1 with respect to the plasma, giving rise to lengthy expressions. For simplicity we give the expression corresponding to the narrow-resonance limit $\Gamma_{N_1} \to 0$, which is always valid. In fact, if the N_1 Yukawa coupling is large, N_1 gets a thermal mass avoiding $H \to N_1 L$ decays.

The reduced $LH \leftrightarrow \bar{L}H^\dagger$ cross section is given by

$$\begin{aligned}\hat{\sigma}^{\rm sub}_{Ns} &= \frac{(Y_\nu Y_\nu^\dagger)^2_{11}}{4\pi x}\Bigg[(1+(1-2a_H+x)({\rm Re}D_{N_1}-3\xi))\ln\left(\frac{R_2^2/x^2+\epsilon}{R_1^2+\epsilon}\right)+ \\ &+\frac{1}{x^2}(a_H^2+(a_L-x)^2-2a_H(a_L+x))\Bigg(|D^2_{N_1}|^{\rm sub}R_2^2+2x{\rm Re}D_{N_1}+ \\ &\frac{2(1+x-2a_H)R_2R_1}{[R_2^2/x^2+\epsilon][R_1^2+\epsilon]}-3\xi(2x+(x-a_H+a_L)^2({\rm Re}D_{N_1}-\xi)\Bigg)\Bigg]\end{aligned} \tag{76}$$

where $R_1 = 1-2a_H-2a_L+x$ and $R_2 = x-(a_H-a_L)^2$ and ϵ is any small number, $\epsilon \ll a_L^2$.

For the $\Delta L = 2$ scattering $LL \leftrightarrow HH$ we obtain

$$\hat{\sigma}_{Nt} = \frac{(Y_\nu Y_\nu^\dagger)^2_{11}}{2\pi}\frac{x-2a_L}{x}\left[\frac{r}{R_1+(a_H-a_L)^2}+\frac{3}{2}r\xi^2+(\frac{1}{R_1+1}+3\xi)\ln\frac{R_1+1+r}{R_1+1-r}\right] \tag{77}$$

where $r \equiv \sqrt{(x-4a_H)(x-4a_L)}$. The parameter ξ takes into account scatterings mediated by heavier right-handed neutrinos $m_{N_{2,3}} \gg m_{N_1}$, as explained in section 4.

$\Delta L = 1$ scatterings

Let us now consider the $\Delta L = 1$ processes $LN \leftrightarrow Q_3U_3$ and $\bar{U}_3N \leftrightarrow Q_3\bar{L}$ (bottom row of fig. 4). We can neglect the small difference between the thermal masses of Q_3 and U_3 (see fig. 1a), setting $a_U \approx a_Q$. The $LN \leftrightarrow Q_3U_3$ reduced cross section is

$$\hat{\sigma}_{Hs} = \frac{3}{4\pi}(Y_\nu Y_\nu^\dagger)_{11}y_t^2\frac{(x-1-a_L)(x-2a_Q)}{x(x-a_H)^2}\sqrt{[(1+a_L-x)^2-4a_L][1-4a_Q/x]}. \tag{78}$$

The $\bar{U}_3N \leftrightarrow Q_3\bar{L}$ and the $\bar{Q}_3N \leftrightarrow U_3\bar{L}$ cross sections are equal and given by

$$\begin{aligned}\hat{\sigma}_{Ht} &= \frac{3}{4\pi}(Y_\nu Y_\nu^\dagger)_{11}y_t^2\frac{1}{x}\Bigg[t_+-t_--(1-a_H+a_L)(a_H-2a_Q)\left(\frac{1}{a_H-t_+}-\frac{1}{a_H-t_-}\right)+ \\ &-(1-2a_H+a_L+2a_Q)\ln\frac{t_+-a_H}{t_--a_H}\Bigg]\end{aligned} \tag{79}$$

where

$$\begin{aligned}t_\pm &\equiv \frac{1}{2x}\Bigg[a_Q+x-(a_Q-x)^2+a_L(x+a_Q-1)+ \\ &\pm\sqrt{[a_Q^2+(x-1)^2-2a_Q(1+x)][a_L^2+(x-a_Q)^2-2a_L(x+a_Q)]}\Bigg]\end{aligned} \tag{80}$$

Neglecting thermal masses, all these interaction rates agree with those used in the literature (up to typos present in older papers). As explained in the text, we must include $\Delta L = 1$ scatterings involving gauge bosons. We do not compute the full thermally corrected rates, since we should take into account thermal motion of A and L with respect to the plasma, which gives a complicated result. We cannot fully neglect thermal effects, since

exchange of massless H and L would give an IR divergent result. Therefore we keep thermal masses of A, L, H only when they act as regulators of IR enhanced contributions. This approximation is accurate at $T \ll m_{N_1}$. At larger T it neglects terms suppressed by higher powers of $g^2 \sim 1/3$. The result is

$$\begin{aligned}
\hat{\sigma}(N_1\bar{L} \to HA) &= \frac{3g_2^2(Y_\nu Y_\nu^\dagger)_{11}}{16\pi x^2}\Big[2t(x-2) + (2-2x+x^2)\ln[(a_L-t)^2+\epsilon] + \\
&\qquad +2\frac{x(a_L-t)(a_L+a_L x-a_W)+\epsilon(2-2x+x^2)}{(a_L-t)^2+\epsilon}\Big]_{t_-}^{t_+} \qquad (81)\\
\hat{\sigma}(LH \to N_1 A) &= \frac{3g_2^2(Y_\nu Y_\nu^\dagger)_{11}}{8\pi x(1-x)}\Big[2x\ln(t-a_H) - (1+x^2)\ln(t+x-1-a_W-a_H)\Big]_{t_-}^{t_+}\\
\hat{\sigma}(\bar{L}A \to N_1 H) &= \frac{3g_2^2(Y_\nu Y_\nu^\dagger)_{11}}{16\pi x^2}\Big[t^2 + 2t(x-2) - 4(x-1)\ln(t-a_H) + x\frac{a_W-4a_H}{a_H-t}\Big]_{t_-}^{t_+}
\end{aligned}$$

We wrote only the $\mathrm{SU}(2)_L$ contribution. One must add the $\mathrm{U}(1)_Y$ contribution, obtained by substituting $a_W \to a_Y$ and $\frac{3}{2}g_2^2 \to \frac{1}{4}g_Y^2$.[13] The expression $[f(t)]_{t_-}^{t_+}$ denotes $f(t_+/m_{N_1}^2) - f(t_-/m_{N_1}^2)$ where $t_\pm$ are the usual kinematical ranges for $t = (P_1 - P_3)^2$ in the various $12 \to 34$ scatterings:

$$t_\pm = \frac{(m_1^2 - m_2^2 - m_3^2 + m_4^2)^2}{4s} - \left(\sqrt{\frac{(s+m_1^2-m_2^2)^2}{4s} - m_1^2} \pm \sqrt{\frac{(s+m_3^2-m_4^2)^2}{4s} - m_3^2}\right)^2$$

In some parameter range the process $N_1\bar{L} \to HA$ can have on-shell L in the t-channel, that we have subtracted: in such a case one should use any finite value $\epsilon \ll a_L^2$. Otherwise one can set $\epsilon = 0$.

The rates that enter in Boltzmann equations are given by

$$\hat{\sigma}_{As} = \hat{\sigma}(LN_1 \to \bar{H}A), \qquad \hat{\sigma}_{At} = \frac{1}{2}\left[\hat{\sigma}(A\bar{L} \to N_1 H) + \hat{\sigma}(\bar{H}\bar{L} \to N_1 A)\right]$$

Resonances in s and u channels

We here explicitly verify that the relation between decay and resonant scatterings, $\gamma_N^{\text{on-shell}} = \gamma_D/4$ (up to CP-violating corrections), remains valid without approximating thermal distributions with Boltzmann statistics, and that it applies to both s-channel as well as u-channel resonances. This last issue is non-trivial, as computing a cross section mediated by an unstable particle which can be on-shell is a difficult problem even at zero

[13] Gauge scatterings have been estimated in a recent paper [29], by introducing some infra-red cutoff, which should give a qualitatively correct result at low temperature. We can only compare the ratio between $\mathrm{SU}(2)_L$ and $\mathrm{U}(1)_Y$ contributions, which is different from our value. We do not use simplified expressions for $t_\pm$, valid when $m_{L,W,H}^2 \ll s, m_{N_1}^2$, because they not even accurate at low temperature, where small $s - m_{N_1}^2 \simeq m_{L,W,H}^2$ is a relevant kinematical range. Due to the $1-x$ factor, at $T \ll m_{N_1}$ the $LH \to N_1 A$ interaction rate is $\gamma_{At} \sim (g/\pi)^2\gamma_D$, of the same order as one loop corrections to the decay rate (that we do not include).

temperature and at tree level. In that case, the beam size and the width of the external unstable particle act as a regulator of the divergence [57].

We first consider the s-channel case. The $N_1 \leftrightarrow LH$ rates are

$$\gamma^{\rm eq}(N_1 \to LH) = \int d\vec{p}_{N_1} d\vec{p}_L d\vec{p}_H \; f_{N_1}(1-f_L)(1+f_H)\,(2\pi)^4\delta^4(P_{N_1}-P_L-P_H)|A(N_1\to LH)|^2$$
$$\gamma^{\rm eq}(LH \to N_1) = \int d\vec{p}_{N_1} d\vec{p}_L d\vec{p}_H \; f_L f_H(1-f_{N_1})\,(2\pi)^4\delta^4(P_{N_1}-P_L-P_H)|A(LH\to N_1)|^2.$$

Using $E_{N_1} = E_H + E_L$, we obtain $f_{N_1}(1-f_L)(1+f_H) = f_L f_H(1-f_{N_1}) = f_L f_{N_1} f_H e^{E_{N_1}/T}$. The on-shell contribution to the $LH \to \bar{L}\bar{H}$ equilibrium interaction rate is

$$\gamma^{\rm eq}_{\rm on-shell}(LH \to \bar{L}\bar{H}) = \int d\vec{p}_H d\vec{p}_L d\vec{p}_{\bar{L}} d\vec{p}_{\bar{H}} \; f_L f_H(1-f_{\bar{L}})(1+f_{\bar{H}})|A(LH\to N_1)|^2$$
$$\left(\frac{\pi\delta(s-m_{N_1}^2)}{m_{N_1}\Gamma^{\rm th}_{N_1}}\right)|A(N_1\to \bar{L}\bar{H})|^2(2\pi)^4\delta^4(P_L+P_H-P_{\bar{L}}-P_{\bar{H}})$$

where the width that cutoffs the resonance is $\Gamma^{\rm th}_{N_1}$ [56], the damping rate at finite temperature. We can rewrite the product of thermal distributions as:

In an analogous way we can deal with u-channel resonance, present in $LH \to \bar{L}\bar{H}$ scatterings at high temperatures when H decays to $N_1\bar{L}$ while N_1 is stable. At finite T the propagator of a particle involved in a $1 \leftrightarrow 2$ process gets an imaginary part, even if it is not the decaying particle. This thermal Γ_{N_1} cutoffs the u-channel resonance and gives consistent Boltzmann equations (no $\mathcal{L}$ asymmetry generated in thermal equilibrium). To show this fact we follow the same procedure. The interaction rates for $\bar{H} \leftrightarrow N_1 L$ are

$$\gamma^{\rm eq}(\bar{H} \to N_1 L) = \int d\vec{p}_{\bar{H}} d\vec{p}_L d\vec{p}_{N_1} \; f_{\bar{H}}(1-f_{N_1})(1-f_L)\,(2\pi)^4\delta^4(P_{\bar{H}}-P_L-P_{N_1})|A(\bar{H}\to LN_1)|^2$$
$$\gamma^{\rm eq}(N_1 L \to \bar{H}) = \int d\vec{p}_{N_1} d\vec{p}_L d\vec{p}_{\bar{H}} \; f_L f_{N_1}(1+f_{\bar{H}})\,(2\pi)^4\delta^4(P_{\bar{H}}-P_L-P_{N_1})|A(N_1 L\to \bar{H})|^2.$$

Since $E_{\bar{H}} = E_{N_1} + E_L$ one can show that $f_{\bar{H}}(1-f_{N_1})(1-f_L) = f_L f_{N_1}(1+f_{\bar{H}})$, so that, again

$$\gamma^{\rm eq}(\bar{H} \to N_1 L) = \gamma^{\rm eq}(N_1\bar{L} \to H) = \frac{\gamma_D}{2}(1+\epsilon_H) \tag{82}$$
$$\gamma^{\rm eq}(N_1 L \to \bar{H}) = \gamma^{\rm eq}(H \to N_1 L) = \frac{\gamma_D}{2}(1-\epsilon_H) \tag{83}$$

where now

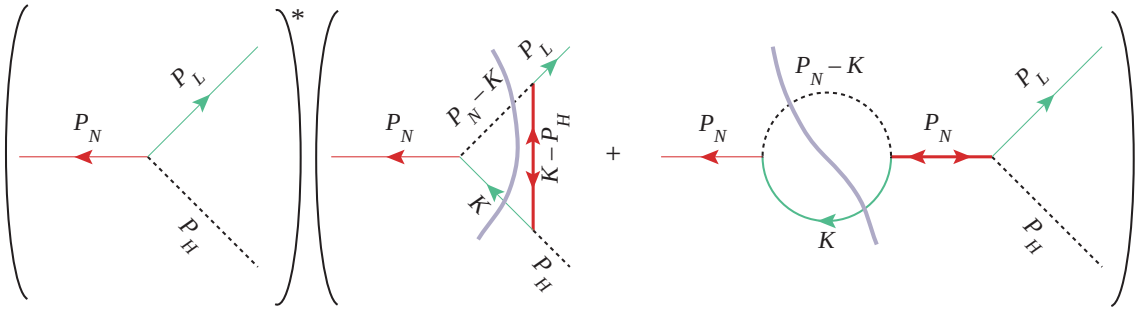

Figure 16: *$Im[I_0^*(I_1^V + I_1^W)]$ in $N_1 \to LH$ decay. The momenta flow in the direction in which the labels are written.*

C Thermal correction to SM CP-asymmetries

In this appendix we show explicitly the calculation of the CP asymmetry parameter ϵ for both the N_1 decay and the H decay, in the SM. Since the final result for leptogenesis turns out to be very weakly dependent on ϵ_H, we compute ϵ_H neglecting the motion of H with respect to the plasma. On the contrary we make the analogous approximation for ϵ_{N_1} only in the analytic expression presented in the main text, eq. (29), and present here the full result, averaged over thermal N_1 motion.

We choose to work in the rest system of the plasma. The CP-asymmetry in $i \to f$ decays which enters into the Boltzmann equations is (see eq. (62))

$$\epsilon_i = \frac{\gamma^{\rm eq}(i \to f) - \gamma^{\rm eq}(\bar{i} \to \bar{f})}{\gamma^{\rm eq}(i \to f) + \gamma^{\rm eq}(\bar{i} \to \bar{f})} = \frac{\int d^3p_i\, f(E_i) \int d\phi\, \epsilon_A |A|^2}{\int d^3p_i\, f(E_i) \int d\phi\, |A|^2} + \mathcal{O}(\epsilon_i^2) \tag{84}$$

where $d^3p_i\, f(E_i)$ is the thermal distribution of the initial state, $d\phi$ is the standard relativistic phase-space for $i \to f$ decay,

$$\epsilon_A = \frac{|A(i \to f)|^2 - |A(\bar{i} \to \bar{f})|^2}{|A(i \to f)|^2 + |A(\bar{i} \to \bar{f})|^2}\,, \tag{85}$$

and A is the amplitude for the process computed at given quadri-momenta $P_{i,f}$. We define $A_0(i \to f)$ as the amplitude of the tree level process and parametrize it as $A_0 = \lambda_0 I_0$, where λ_0 contains the coupling constants. In the same way we define the amplitude up to the one-loop level as $A = \lambda_0 I_0 + \lambda_1 I_1$. With this notations ϵ_A at one-loop is expressed as

$$\epsilon_A = \frac{|\lambda_0 I_0 + \lambda_1 I_1|^2 - |\lambda_0^* I_0 + \lambda_1^* I_1|^2}{|\lambda_0 I_0 + \lambda_1 I_1|^2 + |\lambda_0^* I_0 + \lambda_1^* I_1|^2} \simeq -2 \frac{{\rm Im}[\lambda_0^* \lambda_1]}{|\lambda_0|^2} \frac{{\rm Im}[I_0^* I_1]}{|I_0|^2}\,. \tag{86}$$

In our case I_1 is the sum of two diagrams: a "vertex" correction and a "wave" correction (fig.s 16, 17). For both diagrams the couplings and the $|A_0(i \to f)|^2$ factor are the same:

$$\epsilon_A = -2 \frac{{\rm Im}[(Y^\dagger Y)^2_{1j}]}{(Y^\dagger Y)_{11}} \frac{{\rm Im}[I_0^* I_1]}{2 P_N \cdot P_L} \tag{87}$$

where the quadri-momenta P_N and P_L are defined in fig. 16 for N_1 decay and in fig. 17 for H decay. We have to compute $\mathrm{Im}[I_0^* I_1]$. Using the cutting rules, we obtain

$$\mathrm{Im}[I_0^* I_1] = \frac{1}{2i} I_0 \sum_{\text{cuttings}} I_1 \,. \tag{88}$$

I_1 is the sum of two diagrams: the "vertex" and the "wave" one: $I_1 = I_1^V + I_1^W$.

Computation of ϵ_{N_1}

We consider here the case of $N_1 \to LH$. In principle there are three possible cuttings (or six circlings in the notation of ref. [58, 24]) for I_1^V, and one (or two circlings) for I_1^W, and none of them is forbidden at finite T. In fact, at finite T, energy is no more forced to flow from uncircled to circled vertices (see ref. [24]). The reason is that, while the cut propagators at zero T are proportional to $\theta(E)$, at finite T they have a new contribution, see eqs. (10)–(24), proportional to f_F (or f_B) if the cut particle is a fermion (or a boson). This accounts for particles in the thermal bath which do not have the $\theta(E)$ function, since they can be emitted by the bath (positive energy) or absorbed from the bath (negative energy). However, recalling that we are working under the assumption that the N_j (with $j \neq 1$) are very heavy, the cuttings which involve the N_j can be neglected since they are exponentially suppressed by m_{N_j}/T. Moreover the graph with the N_1 circulating in the loop does not contribute to the CP asymmetry since its Yukawa couplings are real (see eq. (87) with $j = 1$). So, the only relevant cutting in I_1^V is the one with lepton line and Higgs line cut (fig. 16), as in the zero-temperature case.

We compute here the cutting in the vertex part

$$\mathrm{Im}[I_0^* I_1^V] = \frac{1}{2i} \int \frac{d^4K}{(2\pi)^4} D_N(P_L - P_N + K) \left[D_H^+(P_N - K) D_L^+(K) + D_H^-(P_N - K) D_L^-(K) \right] T(K), \tag{89}$$

which is the first contribution shown in fig. 16 (the single cutting in the figure stands for two possible circlings of the vertices). Here $T(K)$ is the result of the traces over the spinor indices, D are the propagators (without numerators): D_N is the propagator of the N_j (which we choose as the zero-temperature one, since we neglect N_j interactions with the plasma), $D_H^\pm$ and $D_L^\pm$ are the finite-T cut propagators of the Higgs and of the lepton respectively, see eq. (10) and (24),

$$\begin{aligned} D_N(P_L - P_N + K) &= \frac{1}{(P_L - P_N + K)^2 - m_{N_j}^2} \\ D_H^\pm(P_N - K) &= 2\pi\delta\big((P_N - K)^2 - m_H^2\big) \left[\theta(\pm(E_N - \omega)) + f_B(|E_N - \omega|)\right] , \\ D_L^\pm(K) &= 2\pi\delta\big(\delta_L(\omega, k)\big) \left[\theta(\pm\omega) - f_F(|\omega|)\right] , \end{aligned} \tag{90}$$

where

$$\delta_L = [(1+a)\omega + b]^2 - (1+a)^2 k^2 \tag{91}$$

and a, b are defined in eq. (16). Keeping only relative angles relevant for our computation, we can conveniently parameterize the quadri-vectors as

$$U = (1,0,0,0), \qquad P_N = (E_N, p_N, 0, 0), \qquad P_H = P_N - P_L = (E_H, \vec{p}_H)$$

$$P_L = ((E_L^0 E_N + p_0 p_N \cos\theta_0)/m_{N_1}, (p_0 E_N \cos\theta_0 + E_L^0 p_N)/m_{N_1}, p_0 \sin\theta_0, 0) = (E_L, \vec{p}_L)$$

$$K = (\omega, k\cos\theta, k\sin\theta\cos\varphi, k\sin\theta\sin\varphi) = (\omega, \vec{k})$$

where $E_L^0 = (m_{N_1}^2 + m_L^2 - m_H^2)/2m_{N_1}$ and $p_0 = \sqrt{(E_L^0)^2 - m_L^2}$ are the L energy and momentum with respect to the N rest frame and θ_0 is a decay angle in the same frame.

Now we compute the trace part. Using four-component Majorana spinors[14], we get

$$T = \sum_{\text{polarizations}} \left[\bar{u}_L \left(i\frac{1-\gamma_5}{2}\right) C\bar{v}_{N_1}\right]^* \left[\bar{u}_L \left(i\frac{1-\gamma_5}{2}\right)\Big(- i[\not{K} - \not{P}_H + m_{N_j}]C\Big)\times\right.$$

$$\left.\times\left(i\frac{1-\gamma_5}{2}\right)\Big(- i\left[(1+a)\not{K} + b\not{\psi}\right]\Big)\left(i\frac{1+\gamma_5}{2}\right)\bar{v}_{N_1}\right], \tag{92}$$

where C is the charge conjugation matrix with the properties

$$C\bar{v} = u\ , \quad \{C, \gamma^\mu\} = 0\ , \quad [C, \gamma^5] = 0\,. \tag{93}$$

Then eq. (92) becomes

$$\begin{aligned} T(K) &= -i\ \mathrm{Tr}\left[m_{N_1}\frac{1+\gamma_5}{2}\not{P}_L m_{N_j}[(1+a)\not{K} + b\not{\psi}]\right] \\ &= -2im_{N_1}m_{N_j}[(1+a)\,P_L\cdot K + b\,E_L]\,. \end{aligned} \tag{94}$$

Note that the term $b\not{\psi}$ is not put to zero by chirality projectors unlike a usual mass term.

We have to perform the integral in d^4K in eq. (89). The most convenient technique is to use polar coordinates θ and φ and integrate first in $d\cos\theta$ using the $\delta[(P_N - K)^2 - m_H^2]$ and then integrate in dk using the $\delta[\delta_L(\omega, k)]$. As we discussed in section 3.3, we can approximate the L dispersion relation with $\omega^2 - k^2 = m_L^2$, finding the following solution

$$\cos\theta = \frac{m_H^2 - m_L^2 - m_{N_1}^2 + 2E_N\omega}{2kp_N}\,, \qquad k = \sqrt{\omega^2 - m_L^2}\,. \tag{95}$$

Imposing that $|\cos\theta| \leq 1$ we find that ω must be comprised between two positive values $\omega_{\min}$ and $\omega_{\max}$. This implies that in the arguments of the θ-functions in eq. (89) we have $\omega > 0$ and $E_N - \omega > 0$, so that expanding $D_H^+(P_N - K)D_L^+(K) + D_H^-(P_N - K)D_L^-(K)$ gives

$$\begin{aligned} N &\equiv [1 + f_B(E_N - \omega)][1 - f_F(\omega)] - f_B(E_N - \omega)f_F(\omega) \\ &= 1 + f_B(E_N - \omega) - f_F(\omega) - 2f_B(E_N - \omega)f_F(\omega)\,. \end{aligned} \tag{96}$$

[14]The direction of the arrows for Majorana spinors in fig. 16 is arbitrary, and one is free to choose it as a matter of convenience; the particular choice made dictates which Feynman rules are used.

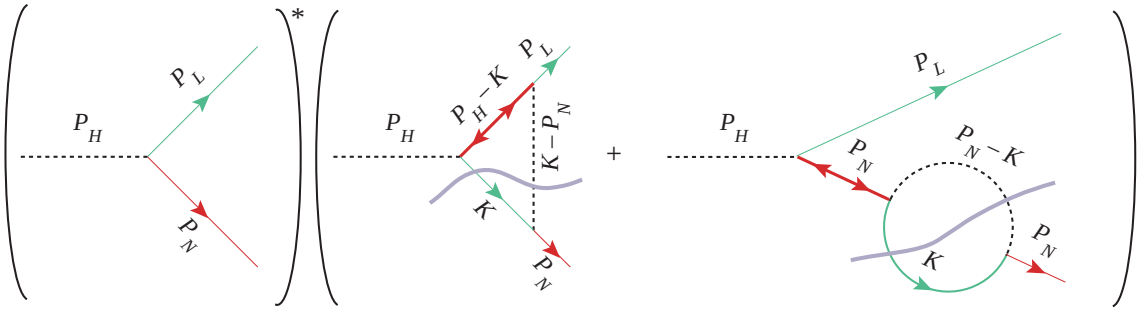

Figure 17: *$Im[I_0^* I_1]$ in $H \to LN$ decay.*

At this point we are left with integrals in $d\omega$ and $d\varphi$. Adding also the contribution of the "wave" diagram the result is given by

$$\epsilon_A = \frac{\mathrm{Im}[(Y^\dagger Y)^2_{1j}]}{2\pi (Y^\dagger Y)_{11}\ |I_0|^2} \int_0^{2\pi} \frac{d\varphi}{2\pi} \int_{\omega_{\min}}^{\omega_{\max}} d\omega \frac{k m_{N_1} m_{N_j}}{|\partial\delta_L/\partial k|\, p_N} [(1+a) P_L \cdot K + b E_L]\, N\, [P_V + 2P_W]\,, \tag{97}$$

where

$$|I_0|^2 = 2P_N \cdot P_L = m_{N_1}^2 - m_H^2 + m_L^2. \tag{98}$$

P_V and P_W arise from N_j propagators in vertex and wave diagrams respectively

$$P_V = \frac{1}{m_H^2 + m_L^2 - m_{N_j}^2 - 2P_H \cdot K}\,, \qquad P_W = \frac{1}{m_{N_1}^2 - m_{N_j}^2}. \tag{99}$$

P_W appears in eq. (97) multiplied by a factor 2 since in the wave diagram also the charged states of Higgs and lepton fields can propagate [25]. Finally, the relevant quantity for the Boltzmann equations is the average of ϵ_A over the phase space and the thermal distribution of N_1:

$$\epsilon_{N_1}(T) = \frac{\int_{m_{N_1}}^\infty dE_N\, p_N\ f_B(E_N) \int_{-1}^1 d\cos\theta_0\ \epsilon_A(E_N, \theta_0)}{2\int_{m_{N_1}}^\infty dE_N\, p_N\ f_B(E_N)}\,. \tag{100}$$

The result is presented in fig. 6. In the limit $m_{N_j} \gg m_{N_1}$ one has $P_V \approx P_W \approx -1/m_{N_j}^2$ and the integrals in φ and θ_0 can be done analytically. Approximating $f_B(E_N) \approx e^{-E_N/T}$ the explicit result is

$$\epsilon_{N_1}(T)\epsilon_{N_1}(0) = \int_{m_{N_1}}^\infty dE_N \int_{\omega_{\min}}^{\omega_{\max}} d\omega\, [(1+a)(m_{N_1}^2 - m_H^2 + m_L^2) + 2bE_N] \frac{2k m_{N_1} N\, e^{-E_N/T}}{T\, \mathrm{K}_1(m_{N_1}/T) |\partial\delta_L/\partial k|}.$$

Computation of ϵ_{N_1} for N_1 at rest

We have then performed the computation for the N_1 decay in the simplified situation with N_1 at rest in the plasma. In this case, the $\delta((P_N - K)^2 - m_H^2)$ factor does not contain the angle θ in the scalar product $P_N \cdot K$. So we can proceed by integrating in dk and in $d\omega$ using the two δ-functions. Moreover there is no dependence on the angles φ and θ_0. The integrals in $d\varphi$ and $d\cos\theta_0$ are trivial and the integral in $d\cos\theta$ can be done analytically. In this way one obtains the result of section 3.3. The difference with respect to our full computation is not fully negligible, as shown in fig. 6a.

Computation of ϵ_H

Finally, the same technique of computation can be applied to the case of $H \to LN_1$. There are, though, remarkable differences between the two decays. In H decay (see fig. 17) the particles in the loop could never go on-shell with the usual $T = 0$ Feynman rules. This is due to the presence of the θ-functions in the cut propagators. However, using the finite-T rules we know that particles with negative energy can be absorbed from the bath so the process can have a CP asymmetry. We can make the cuts in fig. 17, where again cuts of very heavy particles have been neglected. The δ-functions have solutions identical to eq. (95), in terms of the external momenta (see the notation of fig. 17). However the masses are such that $\omega_{\min} < \omega_{\max} < 0$. So imposing $|\cos\theta| \leq 1$, ω has to lie between two *negative* values (it is exactly for this reason that with $T = 0$ Feynman rules ϵ_H would be zero), while $E_N - \omega$ is positive. Then the products of θ-functions are different from the previous case

$$\begin{aligned} & D_H^+(P_N - K)D_L^+(K) + D_H^-(P_N - K)D_L^-(K) \propto \\ & \quad \propto [f_B(|E_N - \omega|)][1 - f_F(|\omega|)] - [1 + f_B(|E_N - \omega|)]f_F(|\omega|) \\ & \quad = f_B(|E_N - \omega|) - f_F(|\omega|) - 2f_B(|E_N - \omega|)f_F(|\omega|). \end{aligned} \tag{101}$$

Indeed eq. (101) is equal to 0 (and not to 1) at $T = 0$.

The result in this case has the same form of eq. (97). As already explained, since the final effect of ϵ_H in our scenario is very small, we computed it only taking the incoming H at rest, in order to simplify the computations. However, in this case it is not possible to give an analytic result as opposed to the case of N_1 decay at rest. The reason is that this time the $\delta((P_N - K)^2 - m_H^2)$ factor contains always the dependence on the angle θ, since N_1 is the outgoing particle and P_N is not of the form $P_N = (m_{N_1}, 0, 0, 0)$.

The most convenient order of integration is the same we followed in the N_1 decay. We obtain again a result in an implicit form (even if there is no dependence on α and φ)

$$\begin{aligned} \epsilon_H(T) = \frac{\mathrm{Im}[(Y^\dagger Y)^2_{1j}]}{(Y^\dagger Y)_{11}|I_0|^2} \cdot 2\pi \int_{q_m}^{q_M} d\omega \frac{m_{N_1} m_{N_j}}{|\partial\delta_L/\partial k|(2\pi)^2} \; [(1+a)\,(E_L\omega - p_L k\cos\theta) + bE_L] \\ \times [f_B(|E_N - \omega|) - f_F(|\omega|) - 2f_B(|E_N - \omega|)f_F(|\omega|)][P_V(\omega) + 2P_W(\omega)]\,, \end{aligned} \tag{102}$$

where δ_L is given by eq.(91) and I_0 is the tree level rate for this decay

$$|I_0|^2 = m_H^2 - m_{N_1}^2 - m_L^2. \tag{103}$$

The on-shell conditions fix

$$k = \sqrt{\omega^2 - m_L^2}\,, \qquad \cos\theta = \frac{m_{N_1}^2 + m_L^2 - m_H^2 - 2E_N\omega}{2p_N k}.$$

Finally $P_V(\omega)$ and $P_W(\omega)$ in this case are given by

$$P_V(\omega) = \frac{k}{p_N\,\left({m_H}^2 + {m_L}^2 - {m_{N_j}}^2 - 2\,m_H\,\omega\right)}\,, \tag{104}$$

$$P_W(\omega) = \frac{k}{p_N\,\left({m_{N_1}}^2 - {m_{N_j}}^2\right)}\,. \tag{105}$$

Note that the tree level rate for this process in eq.(103) is small at high T as long as the value of m_H is near to m_L. For this reason ϵ_H is bigger than ϵ_{N_1}. In fact if $|I_0|^2$ were $\mathcal{O}(1)T^2$ at high T, then ϵ_H would be as big as ϵ_{N_1}. Instead, it goes like cT^2, where c is a small number: $c = (m_H^2 - m_L^2)/T^2$, and so ϵ_H becomes c^{-1} times bigger than ϵ_{N_1}. In particular for the SM thermal masses c^{-1} is about 15.

D Thermal correction to MSSM CP-asymmetries

In the MSSM the situation becomes more complicated than in the SM because we must study both N_1 and $\tilde{N}_1$ decays, each having two possible decay channels, with each channel having more diagrams. Including thermal effects, the relevant masses satisfy

$$m_{N_{1,2,3}} = m_{\tilde{N}_{1,2,3}}, \qquad a_{\tilde{H}} \equiv \frac{m_{\tilde{H}}^2}{m_{N_1}^2} = \frac{a_H}{2}, \qquad a_{\tilde{L}} \equiv \frac{m_{\tilde{L}}^2}{m_{N_1}^2} = 2a_L.$$

As previously discussed we use approximate dispersion relations for the fermions, and assume $m_{N_j} \gg m_{N_1}$. For simplicity, in the MSSM case we compute the decay rates and the CP-asymmetries neglecting the velocity of the decaying particle with respect to the plasma.

The CP-asymmetries in N_1 and $\tilde{N}_1$ decays are

$$\begin{aligned}
\epsilon_{\tilde{N}_1}(T) &\equiv \frac{\Gamma(\tilde{N}_1 \to H\tilde{L}) - \Gamma(\tilde{N}_1 \to \bar{H}\bar{\tilde{L}}) + \Gamma(\tilde{N}_1 \to \tilde{H}L) - \Gamma(\tilde{N}_1 \to \bar{\tilde{H}}\bar{L})}{\Gamma(\tilde{N}_1 \to H\tilde{L}) + \Gamma(\tilde{N}_1 \to \bar{H}\bar{\tilde{L}}) + \Gamma(\tilde{N}_1 \to \tilde{H}L) + \Gamma(\tilde{N}_1 \to \bar{\tilde{H}}\bar{L})} \\
&= \epsilon_{\tilde{N}_1}(T=0)\frac{R_\Gamma(\tilde{N}_1 \to \tilde{H}L)R_\epsilon(\tilde{N}_1 \to \tilde{H}L) + R_\Gamma(\tilde{N}_1 \to H\tilde{L})R_\epsilon(\tilde{N}_1 \to H\tilde{L})}{R_\Gamma(\tilde{N}_1 \to \tilde{H}L) + R_\Gamma(\tilde{N}_1 \to H\tilde{L})} \\
\epsilon_{N_1}(T) &= \epsilon_{N_1}(T=0)R_\epsilon(N_1 \to HL) = \epsilon_{N_1}(T=0)R_\epsilon(N_1 \to \tilde{H}\tilde{L})
\end{aligned}$$

where

$$R_\Gamma(i \to f) \equiv \frac{\Gamma(i \to f \text{ at } T)}{\Gamma(i \to f \text{ at } T=0)} \qquad R_\epsilon(i \to f) \equiv \frac{\epsilon(i \to f \text{ at } T)}{\epsilon(i \to f \text{ at } T=0)}.$$

We have used the fact that at $T = 0$ the two decay channels have equal zero-temperature width and CP-asymmetries $\epsilon_{N_1}(T = 0) = \epsilon_{\tilde{N}_1}(T = 0)$ given in eq. (43).

We now give the explicit expressions for the R_ϵ. Consider first the N_1 decays. Two more one loop diagrams (not plotted) contribute to the CP-asymmetry: a "vertex" and a "wave" diagram with sparticles in the loop. The SM function $R_\epsilon(N_1 \to HL)$ has been given in section 3.3. Using analogous self-explanatory notations we find, in the MSSM

$$\begin{aligned} R_\epsilon(N_1 \to HL) &= 8\frac{k_L^2}{m_{N_1}}[\omega_L(1+a_L)+b_L][1+f_H-f_L-2f_Hf_L]\left|\left|\begin{matrix}\partial\delta_H/\partial\omega_L & \partial\delta_L/\partial\omega_L\\ \partial\delta_H/\partial k_L & \partial\delta_L/\partial k_L\end{matrix}\right|\right|^{-1} + \\ & 8\frac{k_{\tilde{H}}^2}{m_{N_1}}[\omega_{\tilde{H}}(1+a_{\tilde{H}})+b_{\tilde{H}}][1+n_{\tilde{L}}-n_{\tilde{H}}-2n_{\tilde{L}}n_{\tilde{H}}]\left|\left|\begin{matrix}\partial\delta_{\tilde{L}}/\partial\omega_{\tilde{H}} & \partial\delta_{\tilde{H}}/\partial\omega_{\tilde{H}}\\ \partial\delta_{\tilde{L}}/\partial k_{\tilde{H}} & \partial\delta_{\tilde{H}}/\partial k_{\tilde{H}}\end{matrix}\right|\right|^{-1} \end{aligned}$$

where

$$\begin{aligned} &\delta_H \equiv (m_{N_1}-\omega_L)^2-k_L^2-m_H^2 \qquad && \delta_L \equiv [(1+a_L)\omega_L+b_L]^2-(1+a_L)^2k_L^2 \\ &\delta_{\tilde{L}} \equiv (m_{N_1}-\omega_{\tilde{H}})^2-k_{\tilde{H}}^2-m_{\tilde{L}}^2 && \delta_{\tilde{H}} \equiv [(1+a_{\tilde{H}})\omega_{\tilde{H}}+b_{\tilde{H}}]^2-(1+a_{\tilde{H}})^2k_{\tilde{H}}^2. \end{aligned}$$

$R_\epsilon(N_1 \to \tilde{H}\tilde{L})$ has to be evaluated at the values of k_L and ω_L which solve $\delta_H = \delta_L = 0$, approximatively given by eq. (33), and at the values of $k_{\tilde{H}}$ and $\omega_{\tilde{H}}$ which solve $\delta_{\tilde{H}} = \delta_{\tilde{L}} = 0$, approximatively given by $\omega_{\tilde{H}} = (m_{N_1}^2+m_{\tilde{H}}^2-m_{\tilde{L}}^2)/2m_{N_1}$ and $k_{\tilde{H}} = (\omega_{\tilde{H}}^2-m_{\tilde{H}}^2)^{1/2}$.

Finally $R_\epsilon(N_1 \to \tilde{H}\tilde{L}) = R_\epsilon(N_1 \to HL)$ since the CP-asymmetry in the two N_1 decay modes is due to loops with the same virtual particles.

For $\tilde{N}_1$ decays, the situation is different. When $\tilde{N}_1$ decays into two fermions ($\tilde{N}_1 \to \tilde{H}L$) the imaginary part is obtained cutting two internal bosons, H and $\tilde{L}$. The decay rate is suppressed by two Pauli-blocking factors, but its CP-asymmetry is enhanced by two stimulated-emission factors.

$$R_\epsilon(\tilde{N}_1 \to \tilde{H}L) = 2\frac{k_H}{m_{\tilde{N}_1}}[1+f_B(\omega_{\tilde{L}})+f_B(\omega_H)+2f_B(\omega_{\tilde{L}})f_B(\omega_H)] \tag{106}$$

where $\omega_H = (m_{\tilde{N}_1}^2+m_H^2-m_{\tilde{L}}^2)/2m_{\tilde{N}_1} = m_{\tilde{N}_1}-\omega_{\tilde{L}}$ and $k_H = (\omega_H^2-m_H^2)^{1/2}$.

When $\tilde{N}_1$ decays into two bosons ($\tilde{N}_1 \to H\tilde{L}$) the imaginary part is obtained cutting two internal fermions, $\tilde{H}$ and L, and it is therefore given by a lengthy expression. The CP-asymmetry is suppressed by two Pauli-blocking factors, but the decay rate is enhanced by two stimulated-emission factors.

$$\begin{aligned} R_\epsilon(\tilde{N}_1 \to H\tilde{L}) = 16\frac{k^2}{m_{\tilde{N}_1}^2}\Big\{[(1+a_L)\omega+b_L][(1+a_{\tilde{H}})\omega_{\tilde{H}}+b_{\tilde{H}}]+k^2(1+a_L)(1+a_{\tilde{H}})\Big\}\times \\ \times[1-f_F(m_{\tilde{N}_1}-\omega)-f_F(\omega)+2f_F(m_{\tilde{N}_1}-\omega)f_F(\omega)]\left|\left|\begin{matrix}\partial\delta_L/\partial\omega & \partial\delta_{\tilde{H}}/\partial\omega\\ \partial\delta_L/\partial k & \partial\delta_{\tilde{H}}/\partial k\end{matrix}\right|\right|^{-1} \end{aligned} \tag{107}$$

where (ω, k) is the quadri-momentum of L, $\omega_{\tilde{H}} = m_{\tilde{N}_1}-\omega$ is the energy of $\tilde{H}$ and

$$\delta_{\tilde{H}} \equiv [(1+a_{\tilde{H}})(m_{\tilde{N}_1}-\omega)+b_{\tilde{H}}]^2-(1+a_{\tilde{H}})^2k^2 \qquad \delta_L \equiv [(1+a_L)\omega+b_L]^2-(1+a_L)^2k^2.$$

The expression should be evaluated at the values of ω and k which solve $\delta_L = \delta_{\tilde{H}} = 0$. Using the approximate on-shell condition, they are given by

$$\omega = (m^2_{\tilde{N}_1} + m^2_L - m^2_{\tilde{H}})/2m_{\tilde{N}_1}, \qquad k = (\omega^2 - m^2_L)^{1/2}.$$

Finally, the thermal corrections to the decay rates are given by

$$\begin{aligned}
R_\Gamma(N_1 \to HL) &= (1 + f_B(E_H))(1 - f_F(E_L))\lambda^{1/2}(1, a_H, a_L)(1 - a_H + a_L) \\
R_\Gamma(N_1 \to \tilde{H}\tilde{L}) &= (1 - f_F(E_{\tilde{H}}))(1 + f_B(E_{\tilde{L}}))\lambda^{1/2}(1, a_{\tilde{H}}, a_{\tilde{L}})(1 + a_{\tilde{H}} + a_{\tilde{L}}) \\
R_\Gamma(\tilde{N}_1 \to \tilde{H}L) &= (1 - f_F(E_{\tilde{H}}))(1 - f_F(E_L))\lambda^{1/2}(1, a_{\tilde{H}}, a_L)(1 - a_{\tilde{H}} - a_L) \\
R_\Gamma(\tilde{N}_1 \to H\tilde{L}) &= (1 + f_B(E_H))(1 + f_B(E_{\tilde{L}}))\lambda^{1/2}(1, a_H, a_{\tilde{L}}).
\end{aligned}$$

The $1 \pm f_{B,F}$ factors take into account Pauli blocking or stimulated emission (the thermal distributions must be evaluated at the energies of final state particles) while the other factors arise from thermal corrections to kinematics.

Note added Some of our preliminary results appeared in [49]. However, in that paper sneutrino reheating was not correctly included (we also take into account thermal corrections and proper subtraction of on-shell scatterings).

References

[1] The atmospheric mixing parameters are extracted from the revised SK analysis presented by K. Nishikawa at the 2003 Lepton-Photon Conference (see the web site conferences.fnal.gov/lp2003) and from K2K collaboration, Phys. Rev. Lett. 90 (041801) 2003 [hep-ex/0212007]. For a recent global fit see L. Fogli, E. Lisi, A. Marrone, D. Montanino, A. Palazzo, A.M. Rotunno, hep-ph/0310012. The solar mixing parameters are taken from the global fit in P. Creminelli et al., JHEP 05 (052) 2001 [hep-ph/0102234]. Its e-print version, has been updated including the recent data from SNO (SNO collaboration, nucl-ex/0309004), KamLAND (KamLAND collaboration, hep-ex/0212021), etc.

[2] M. Gell-Mann, P. Ramond and R. Slansky, proceedings of the supergravity Stony Brook workshop, New York, 1979, ed.s P. Van Nieuwenhuizen and D. Freedman (North-Holland, Amsterdam); T. Yanagida, proceedings of the workshop on unified theories and baryon number in the universe, Tsukuba, Japan 1979 (ed.s. O. Sawada and A. Sugamoto, KEK Report No. 79-18, Tsukuba).

[3] M. Fukugita and T. Yanagida, Phys. Lett. B 174, 45 (1986).

[4] For reviews, see A. Riotto, hep-ph/9807454. A. Riotto, M. Trodden, Ann. Rev. Nucl. Part. Sci. 49, 35 (1999).

[5] A. D. Sakharov, Pisma Zh. Eksp. Teor. Fiz. 5, 32 (1967) [JETP Lett. 5, 24 (1967)].

[6] M. A. Luty, Phys. Rev. D 45 (1992) 455; M. Plümacher, Z. Phys. C 74 (1997) 549; W. Buchmuller, M. Plümacher, Int. J. Mod. Phys. A 15, 5047 (2000) [hep-ph/0007176].

[7] R. Barbieri et al., JHEP 10 (1999) 20 [hep-ph/9906470].

[8] T. Hambye, E. Ma, U. Sarkar, Nucl. Phys. B 590 (2000) 429 [hep-ph/0006173]; S. Davidson, A. Ibarra, JHEP 0109 (2001) 013; G.C. Branco, T. Morozumi, B.M. Nobre, M.N. Rebelo, Nucl. Phys. B 617 (2001) 475; A.S. Joshipura, E. A. Paschos, W. Rodejohann, JHEP 0108 (2001) 029; D. Falcone, Phys. Rev. D 66 (2002) 053001 [hep-ph/0204335]; G. C. Branco, R. Gonzalez Felipe, F.R. Joaquim, M.N. Rebelo, Nucl. Phys. B 640 (2002) 202; W. Rodejohann, Phys. Lett. B 542 (2002) 100; J.R. Ellis, M. Raidal, Nucl. Phys. B 643 (2002) 229 [hep-ph/0206174]; G.C. Branco, R. Gonzalez Felipe, F.R. Joaquim, I. Masina, M.N. Rebelo, C.A. Savoy, hep-ph/0211001; S.F. King, hep-ph/0211228; S. Pascoli, S.T. Petcov, C.E. Yaguna, hep-ph/0301095; S. Davidson, JHEP

0303 (2003) 037 [hep-ph/0302075]; E. Kh. Akhmedov, M. Frigerio, A. Yu. Smirnov, hep-ph/0305322.

[9] W. Buchmuller, P. Di Bari, M. Plümacher, Phys. Lett. B 547 (2002) 128 [hep-ph/0209301]; W. Buchmuller, P. Di Bari, M. Plümacher, Nucl. Phys. B 665 (2003) 445 [hep-ph/0302092].

[10] Y. Grossman, T. Kashti, Y. Nir, E. Roulet, hep-ph/0307081.

[11] G. D'Ambrosio, G. F. Giudice, M. Raidal, hep-ph/0308031.

[12] For a review see M. Le Bellac, *Thermal Field Theory*, Cambridge University Press, Cambridge, England, 1996.

[13] P. Elmfors, K. Enqvist, I. Vilja, Nucl. Phys. B **412**, 459 (1994).

[14] V.V. Klimov, Sov. J. Nucl. Phys. 33, 934 (1981); H. A. Weldon, Phys. Rev. D 26, 2789 (1982) and Phys. Rev. D 40, 2410 (1989).

[15] D. J. Gross, R. D. Pisarski, L. G. Yaffe, Rev. Mod. Phys. 53, 43 (1981).

[16] T. Kinoshita, J. Math. Phys. 3, 650 (1962).

[17] T. D. Lee, M. Nauenberg, Phys. Rev. 133, 1549 (1964).

[18] R. D. Pisarski, Phys. Rev. Lett. 63, 1129 (1989); E. Braaten, R. D. Pisarski, Nucl. Phys. B337, 569 (1990); *ibidem* B339, 310 (1990).

[19] H. A. Weldon, Phys. Rev. D 44, 3955 (1991).

[20] K. Kajantie, M. Laine, K. Rummukainen, M. E. Shaposhnikov, Nucl. Phys. B 458 (1996) 90 [hep-ph/9508379].

[21] A. Romanino, A. Strumia, Phys. Lett. B487 (2000) 165 [hep-ph/9912301].

[22] Thermal masses can be found in the several works, after fixing various discrepancies. See refs. [13, 14, 53] and D. Comelli, J. R. Espinosa, Phys. Rev. D 55 (1997) 6253 [hep-ph/9606438].

[23] L. Covi, N. Rius, E. Roulet, F. Vissani, Phys. Rev. D 57 (1998) 93 [hep-ph/9704366].

[24] R. L. Kobes, G. W. Semenoff, Nucl. Phys. B 260 (1985) 714; R. L. Kobes, G. W. Semenoff, Nucl. Phys. B 272 (1986) 329.

[25] L. Covi, E. Roulet, F. Vissani, Phys. Lett. B 384, 169 (1996) [hep-ph/9605319].

[26] R. Barbieri, P. Creminelli, A. Strumia, N. Tetradis, Nucl. Phys. B 575 (2000) 61 [hep-ph/9911315]. The hep-ph version will present revised analytical approximations, in the light of the modified Boltzmann equations discussed here.

[27] S. Davidson, A. Ibarra, Phys. Lett. B 535 (2002) 25.

[28] W. Buchmuller, P. Di Bari, M. Plumacher, Nucl. Phys. B 643 (2002) 367 [hep-ph/0205349].

[29] A. Pilaftsis, T. E. Underwood, hep-ph/0309342.

[30] M. Plümacher, Nucl. Phys. B 530 (1998) 207 [hep-ph/9704231].

[31] F. Borzumati, A. Masiero, Phys. Rev. Lett. 57 (1986) 961; L.J. Hall, V.A. Kostelecky, S. Raby, Nucl. Phys. B267 (1986) 415; J. Hisano, T. Moroi, K. Tobe, M. Yamaguchi, T. Yanagida, Phys. Lett. B357 (1995) 579 [hep-ph/9501407]; J. Hisano, T. Moroi, K. Tobe, M. Yamaguchi, Phys. Rev. D 53 (1996) 2442. For some recent analyses see e.g. J.A. Casas, A. Ibarra, Nucl. Phys. B 618 (2001) 171; S. Davidson, A. Ibarra, hep-ph/0104076; S. Lavignac, I. Masina, C. A. Savoy, Phys. Lett. B520 (2001) 269 [hep-ph/0106245]; J.R. Ellis, J. Hisano, S. Lola, M. Raidal, Nucl. Phys. B 621 (2002) 208 [hep-ph/0109125]; A. Romanino, A. Strumia, Nucl. Phys. B622 (2002) 73 [hep-ph/0108275]; J.R. Ellis, J. Hisano, M. Raidal, Y. Shimizu, Phys. Rev. D 66 (2002) 115013 [hep-ph/0206110]; A. Dedes, J.R. Ellis, M. Raidal, Phys. Lett. B 549, 159 (2002) [hep-ph/0209207].

[32] M. Raidal, A. Strumia, Phys. Lett. B553 (2003) 72 [hep-ph/0210021].

[33] For a review on inflation, see D. H. Lyth, A. Riotto, Phys. Rept. 314, 1 (1999) [hep-ph/9807278].

[34] S. Davidson, M. Losada, A. Riotto, Phys. Rev. Lett. 84, 4284 (2000) [hep-ph/0001301].

[35] G. F. Giudice, E. W. Kolb, A. Riotto, D. V. Semikoz, I. I. Tkachev, Phys. Rev. D 64, 043512 (2001) [hep-ph/0012317].

[36] G. F. Giudice, E. W. Kolb, A. Riotto, Phys. Rev. D 64, 023508 (2001) [hep-ph/0005123].

[37] N. Fornengo, A. Riotto, S. Scopel, Phys. Rev. D 67, 023514 (2003) [hep-ph/0208072].

[38] E. W. Kolb, M. S. Turner, *The Early Universe*, (Addison-Wesley, Menlo Park, Ca., 1990).

[39] D. J. Chung, E. W. Kolb, A. Riotto, Phys. Rev. D 60, 063504 (1999) [hep-ph/9809453].

[40] K. Kumekawa, T. Moroi, T. Yanagida, Prog. Theor. Phys. 92, 437 (1994).

[41] E. W. Kolb, A. D. Linde, A. Riotto, Phys. Rev. Lett. 77, 4290 (1996); E. W. Kolb, A. Riotto, I. I. Tkachev, Phys. Lett. B423, 348 (1998).

[42] G. F. Giudice, M. Peloso, A. Riotto and I. I. Tkachev, JHEP 9908, 014 (1999) [hep-ph/9905242].

[43] E. W. Kolb, A. Notari, A. Riotto, hep-ph/0307241, to be published in Phys. Rev. D.

[44] P. H. Chankowski, K. Turzynski, Phys. Lett. B 570, 198 (2003) [hep-ph/0306059].

[45] J. R. Ellis, J. Kim, D. V. Nanopoulos, Phys. Lett. B145, 181 (1984); L. M. Krauss, Nucl. Phys. B227, 556 (1983); M. Yu. Khlopov, A. D. Linde, Phys. Lett. 138B, 265 (1984); J. R. Ellis, D. V. Nanopoulos, K. A. Olive, S.-J. Rey, Astropart. Phys. 4, 371 (1996); M. Bolz, A. Brandenburg, W. Buchmuller, Nucl. Phys. B 606, 518 (2001).

[46] R. H. Cyburt, J. Ellis, B. D. Fields, K. A. Olive, Phys. Rev. D 67, 103521 (2003).

[47] H. Murayama, H. Suzuki, T. Yanagida, J. Yokoyama, Phys. Rev. Lett. 70 (1993) 1912; H. Murayama, H. Suzuki, T. Yanagida, J. Yokoyama, Phys. Rev. D 50 (1994) 2356 [hep-ph/9311326].

[48] H. Murayama, T. Yanagida, Phys. Lett. B 322 (1994) 349 [hep-ph/9310297]; K. Hamaguchi, H. Murayama, T. Yanagida, Phys. Rev. D 65 (2002) 043512 [hep-ph/0109030]; T. Moroi, H. Murayama, Phys. Lett. B 553 (2003) 126 [hep-ph/0211019].

[49] J. R. Ellis, M. Raidal, T. Yanagida, hep-ph/0303242.

[50] A. Pilaftsis, Phys. Rev. D 56 (1997) 5431 [hep-ph/9707235]; T. Hambye, Nucl. Phys. B 633 (2002) 171 [hep-ph/0111089]; J. R. Ellis, M. Raidal, T. Yanagida, Phys. Lett. B 546, 228 (2002) [hep-ph/0206300].

[51] I. Vysotsky, A. D. Dolgov, Y. B. Zeldovich, Pisma Zh. Eksp. Teor. Fiz. 26, 200 (1977).

[52] E. W. Kolb, S. Wolfram, Nucl. Phys. B 172, 224 (1980) [Erratum-ibid. B 195, 542 (1982)].

[53] J. M. Cline, K. Kainulainen, K. A. Olive, Phys. Rev. D 49, 6394 (1994).

[54] C. Ford, D.R. Jones, P.W. Stephenson, M.B. Einhorn, Nucl. Phys. B395 (1993) 17; A. Sirlin, R. Zucchini, Nucl. Phys. B266 (1986) 389; R. Hempfling, B.A. Kniehl, Phys. Rev. D51 (1995) 1386.

[55] P.H. Chankowski, Z. Pluciennik, Phys. Lett. B316 (1993) 312 [hep-ph/9306333]; K.S. Babu, C.N. Leung, J. Pantaleone, Phys. Lett. B319 (1993) 191 [hep-ph/9309223]. An error has been corrected in S. Antusch, M. Drees, J. Kersten, M. Lindner, M. Ratz, Phys. Lett. B519 (2001) 238 [hep-ph/0108005]. For a recent analysis see S. Antusch, J. Kersten, M. Lindner, M. Ratz, hep-ph/0305273.

[56] Thermal corrections to decay rates have been employed in D.A. Dicus et al., Phys. Rev. D26 (1982) 2694 and formalized in H. A. Weldon, Phys. Rev. D 28, 2007 (1983).

[57] I. F. Ginzburg, Nucl. Phys. Proc. Suppl. 51A (1996) 85 [hep-ph/9601272]; K. Melnikov, G. L. Kotkin, V. G. Serbo, Phys. Rev. D 54 (1996) 3289 [hep-ph/9603352].

[58] Diagrammar, by G. 't Hooft, M.J.G. Veltman, CERN report 73-9 (1973).